MULTI-CHANNEL K-NN CLASSIFICATIONS OF RESPIRATORY SOUNDS

by

Cemile Aslı Yılmaz

B.S. in Electronics & Telecommunication Eng.,

İstanbul Technical University, 1994

Submitted to the Institute for Graduate Studies
in Science and Engineering in partial fulfillment of
the requirements for the degree of
Master of Science

Graduate Program in System Control Engineering

Boğaziçi University

2006

MULTI-CHANNEL K-NN CLASSIFICATIONS OF RESPIRATORY SOUNDS

APPROVED BY :

Assoc. Prof. Yasemin P. Kahya .....
(Thesis Supervisor)

Assoc. Prof. Ayşın Ertüzün .....

Prof. Dr. Fikret Gürgen .....

DATE OF APPROVAL : 15.06.2006

ACKNOWLEDGEMENT

I would like to thank Assoc. Prof. Yasemin P.Kahya for her patient guidance and help throughout this work. Her kindness and permanent support was encouraging and inspiring at all stages of my thesis work.

I would like to thank İpek Şen, R.Koray Çiftçi and Mete Yeğiner for their priceless intention to help whenever I was in need. I have very much benefited from the discussions with them. I will always appreciate their hospitality any time I needed to work in Lung Acoustics Laboratory.

Finally, I would like to thank my mother, Miyase Yılmaz, my father Mehmet Fikret Yılmaz, my sisters Esin Yılmaz Başçeri and Senem Yılmaz for their endless kindness and empathy, and Paco for being a very beautiful part of my life.

ABSTRACT

MULTI-CHANNEL K-NN CLASSIFICATIONS OF RESPIRATORY SOUNDS

Our main interest in this study is to compare two different feature sets derived from respiratory sounds for optimum classification where multi-channel classification algorithm with each channel weighted equally is used. Two class recognition problem made of healthy and pathological sound data is addressed. The performance of our classifier is based on how well it differentiates between healthy and pathological sounds.

For this purpose, parallel recording from 12 microphones placed on the posterior chest were used to extract two different group of sets of features for classification. Respiratory sounds of pathological and healthy subjects were analyzed via frequency spectrum and autoregressive (AR) model parameters.

Since due to the physiology of the lungs, the transmission characteristics and therefore the spectral characteristics differ for respiratory sounds heard at different locations on the chest, separate reference libraries were built for each microphone location. Each subject is represented by 13 channels of respiratory sound data of a single or multiple respiration cycles depending on applied feature extraction methodology. Two reference libraries, pathological and healthy, were built based on multi-channel respiratory sound data for each channel and for each respiration phase, inspiration and expiration, separately. A multi-channel classification algorithm using k nearest neighbor (k-NN) classification method was designed. Performances of the two classifiers using quantile frequencies and AR model parameters as feature sets, are compared separately for inspiration and expiration phases.

ÖZET

ÇOKLU KANALLI SOLUNUM SESİ EN YAKIN KOMŞU SINIFLANDIRMALARI

Bu çalışmada temel amacımız her kanalın eşit ağırlıklı olarak değerlendirildiği çoklu kanallı sınıflandırma algoritmasının farklı iki özellik seti için karşılaştırmasını yapmaktır. Sınıflandırma hastalıklı ve sağlıklı olmak üzere iki grup ses verisi için gerçekleştirilmektedir. Sınıflandırıcının performansı hastalıklı ve sağlıklı sesleri birbirinden ne kadar iyi ayırdedebildiğine bağlıdır.

Bu amaçla, 12 mikrofonun sırta yerleştirilmesi ile paralel kaydedilen solunum sesleri, sınıflandırıcıya temel teşkil edecek özellik setlerini oluşturmak için kullanılmıştır. Hastalıklı ve sağlıklı solunum sesleri frekans spektrumu ve AR modelleme kullanılarak analiz edilmiştir.

Akciğerin fizyolojisi nedeniyle, sırtın farklı noktalarında duyulan solunum sesi, iletim özellikleri, dolayısıyla, spektral özellikleri bakımından farklılaşmaktadır. Bu nedenle referans kütüphaneleri oluşturulurken, sırtta yer alan her mikrofon lokasyonu ayrı özellik kütüphanesi grupları yaratmak için kullanılmıştır. Her denek 12 farklı kanal için, o kanaldan kaydedilmiş olan bir veya birden fazla solunum döngüsü ile temsil edilmiştir. Solunum döngüsünün her kanal için bir veya birden fazla olması özellik çıkarma metodolojisine bağlıdır. Sağlıklı ve hastalıklı şeklinde iki referans kütüphanesi, çoklu kanallı solunum sesini baz alarak, her kanaldaki nefes alma ve verme fazları için ayrı ayrı oluşturulmuştur. En yakın komşuluk sınıflandırıcısı kullanan çoklu kanallı bir sınıflandırıcı kurgulanmıştır. Frekans sıklığı ve AR model parametrelerini özellik seti olarak kullanan iki sınıflandırıcı nefes alma ve verme fazları için ayrı ayrı karşılaştırılmıştır.

TABLE OF CONTENTS

LIST OF FIGURES

LIST OF TABLES

LIST OF SYMBOLS/ABBREVIATIONS

AR	Autoregressive
ARMA	Autoregressive Moving Average
ECG	Electrocardiographic
EEG	Electroencephalographic
EMG	Electromyographic
LPC	Linear Predictive Coding
NN	Nearest Neighbor
PSD	Power Spectral Density

1. INTRODUCTION

1.1. Background

Since the invention of the stethoscope by French physician Reneé Theophil Laënnec, auscultation of pulmonary sounds using a stethoscope is widely used since it is a simple, cheap and patient-friendly method [1].

However, it is regarded as a tool of low diagnostic value due to its subjectivity in evaluating pulmonary sounds, resulting in a large inter subject and intra subject variability and due to its inability to reproduce these findings for comparative assessment since lung sounds show variations, both among different subjects depending on the physiology (age, sex, type and degree of illness etc.) and within an individual, depending on the localization of the auscultation place.

Based on the shortcomings of the method, there has been increased research activity for developing computerized methods for auscultation and diagnosis based on respiratory sounds [2,3,4].

Previous researchs on respiratory sound showed that the power of the normal breath sound signal diminishes as frequency increases [1]. A detailed study on the analysis and comparison of spectral characteristics of the respiratory sounds in healthy and pathological subjects has been carried out by Chowdury and Majumder [5].

Today it is well known that the respiratory sounds include frequencies up to 2000 Hz. The fact that stethoscope attenuates frequency components above 120 Hz and human ear is not very sensitive to frequencies below 120 Hz is another indicator of auscultation weakness in diagnosis [1].

Automation of classification in respiratory sounds becomes an important goal of this research area. For this purpose various approaches including parametric representation of respiratory sound signals have been used [6]. AR modeling method is used to represent

respiratory sound transmission characteristics [7]. Another study [8] performed in this area has used autoregressive model parameters as feature set and k-nearest neighbor classification using Itakura distance measure as classifier.

Over the last 30 years, computerized methods for the analysis of respiratory sound have overcome many limitations of auscultation [9].

1.2. Respiratory Sounds

The breath sounds heard on the chest wall of healthy subjects are called normal breath sounds [1]. Normal breath sound has acoustically a soft character and it consists of different waveforms containing many different frequencies (Figure 1.1) [10]. On the chest wall, it can be characterized by a low noisy sound during inspiration, and it is hardly audible during expiration [11].

The variations occurring in the characteristics of respiratory sounds heard over the chest wall provide the experienced physician important information about the pathological situation [10].

Respiratory sounds are classified roughly into two classes, breath sounds and adventitious sounds. Breath sounds are described as the normal respiratory noise heard on the chest wall and mouth. These are synchronous with the flow of air through the airways. In healthy lungs, breath sounds have a frequency range of 200-600 Hz. Adventitious sounds are additional respiratory sounds superimposed on normal breath sounds and can be discontinuous (crackles) or continuous (wheeze).

Crackles are explosive, transient in character and can be classified as fine (higher pitch) or coarse (lower pitch). As a general rule, their duration is less then 20 ms, with a wide frequency range (100 to 2000 Hz).

Wheeze is a sinusoidal waveform with duration of more than 100 ms, and these are common clinical signs in patients with obstructive airways disease as well as in patients with asthma [10].

Wheezes and crackles are considered to be the parts of the respiratory sound that yield significant clinical information [12]. Thus type of the adventitious sounds, the number of occurrence per one breath and their location within the flow cycle, pitch (for crackles), duration and number of occurrence give valuable information about the type and severity of the disease. Different sample of respiratory sound are depicted in Figure 1.1, [13].

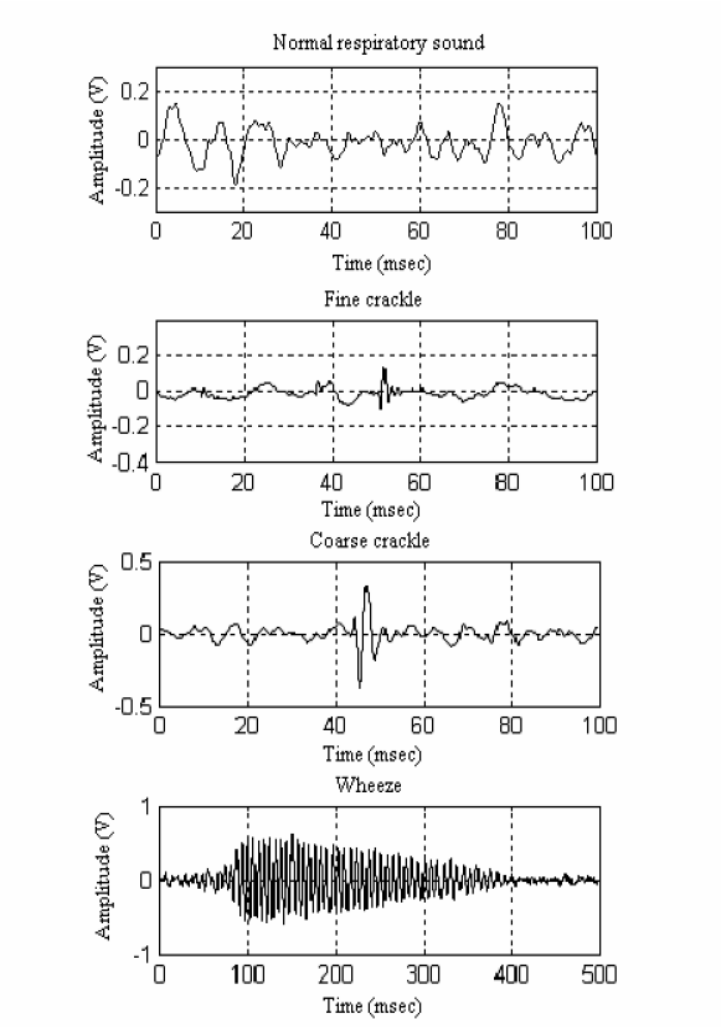

Figure 1.1. Different samples of respiratory sound

1.3. Motivation and Aim

Previously, there have been studies for modeling [7] and for classification [8,14] of respiratory sounds with a view to parameterize these sounds and to make auscultation a more objective and valuable diagnosis tool. In these studies, however, only sound data from one microphone was used in classification and the placement of the microphone on the chest was guided under the supervision of a pulmonary physician such that the microphone was placed on the location where the sound characteristics of the pathological subject varied the most from healthy sound data. In this study, parallel recording from 12 microphones placed on the posterior chest were used to extract two different sets of features for classification. Moreover, since due to the physiology of the lungs, the transmission characteristics and therefore the spectral characteristics differ for respiratory sounds heard at different locations on the chest, separate reference libraries were built for each microphone location both for healthy and pathological data corresponding to inspiration and expiration.

In previous studies [15] k-NN classification algorithm had already applied for one channel respiratory sound classification problem. In this study, also k-NN method is chosen as classifier. By this, the differentiation of the classification results from the previous studies outcomes would be the impact of multi-channel data to classification.

Our main interest is to compare two different feature sets derived from respiratory sounds for optimum classification where multi-channel classification algorithm with each channel weighted equally is used. Two class recognition problem made of healthy and pathological sound data is addressed. The performance of our classifier is based on how well it differentiates between healthy and pathological sounds.

2. SIGNAL PROCESSING

2.1. Introduction

Biomedical signals are signals extracted from biological systems. In signal analysis, modern signal processing techniques are applicable for any kind of biomedical signals. The biomedical signals of common interest are electroencephalographic (EEG), electromyographic (EMG) and electrocardiograhic (ECG) signals that give information about the condition of the related part of the body. Respiratory sound signals are also complex biomedical signals as ECG, EEG or EMG.

Signals are mainly classified into two groups: random and deterministic signals. The difference between them is that deterministic signals can be described in terms of explicit mathematical expression but random signals cannot be exactly expressed, instead statistical averages and probabilities are convenient to describe these signals. Random signals can also be classified into two main groups as nonstationary and stationary signals. Biomedical signals are nonstationary and nonlinear, but with some approximation methods the signal can be treated as stationary signals and signal processing methods for stationary signals can be applied to these signals [15].

2.2. Signal Processing Methods

2.2.1. AR Modeling

A nonstationary signal may be considered stationary for limited time duration so can be divided in time domain into segments that are stationary. The length of the segments depends on the properties of nonstationarities [16]. Parametric modeling is a very common technique in modeling stationary signals. The parameters can be used to process or classify the signal.

The basic formula of the model is as follows:

$$s(n) = -\sum_{i=1}^{p} a_i s(n-i) + \sum_{i=0}^{q} b_i u(n-i) + \sum_{i=0}^{p} c_i \xi(n-i) \tag{2.1}$$

In Equation (2.1), $s(n)$ is sampled signal at time n, output of the linear system at time n, $u(n)$ is input of the linear system and $\xi(n)$ is the additive noise.

The transfer function of this system is the parametric model. In Equation (2.1), additive noise ($\xi(n)$) is considered to be the output of a noise filter having white noise as input $\omega(n)$, thus

$$\sum_{i=1}^{k} c_i \xi(n-i) = \sum_{i=0}^{l} d_i \omega(n-i) \tag{2.2}$$

We can get from Equation (2.1) and Equation (2.2),

$$a(n) = \sum_{i=1}^{p} a_i s(n-i) \tag{2.3}$$

$$b(n) = \sum_{i=0}^{q} b_i u(n-i) \tag{2.4}$$

$$c(n) = \sum_{i=0}^{k} c_i \xi(n-i) \tag{2.5}$$

$$d(n) = \sum_{i=0}^{l} d_i \omega(n-i) \tag{2.6}$$

The z-transform of the definitions in Equation (2.3), Equation (2.4), Equation (2.5) and Equation (2.6) gives us,

$$A\left(z^{-1}\right)=\sum_{i=0}^{p}a_i z^{-i} \quad ; \quad a_0=1 \tag{2.7}$$

$$B\left(z^{-1}\right)=\sum_{i=0}^{q}b_i z^{-i} \tag{2.8}$$

$$C\left(z^{-1}\right)=\sum_{i=0}^{k}c_i z^{-i} \tag{2.9}$$

$$D\left(z^{-1}\right)=\sum_{i=0}^{l}d_i z^{-i} \tag{2.10}$$

From the above equations we have the transfer function model of the system (Figure 2.1);

$$S\left(z\right)=\frac{B\left(z^{-1}\right)}{A\left(z^{-1}\right)}U\left(z\right)+\frac{D\left(z^{-1}\right)}{C\left(z^{-1}\right)}W\left(z\right) \tag{2.11}$$

s(n) can be modeled by system parameter vector $\underline{\beta_s^T}$ and noise parameter vector $\underline{\beta_w^T}$ determined by the following expressions:

$$\underline{\beta_s^T}=\left[a_0,a_1,....,a_{p,}b_0,b_1,....,b_q\right] \tag{2.12}$$

$$\underline{\beta_w^T}=\left[c_0,c_1,....,c_{k,}d_0,d_1,....,d_l\right] \tag{2.13}$$

$\underline{\beta_s^T}$ describes a linear transformation of the white noise sequence into signal sequence if $u(n)$ is assumed to be white noise.

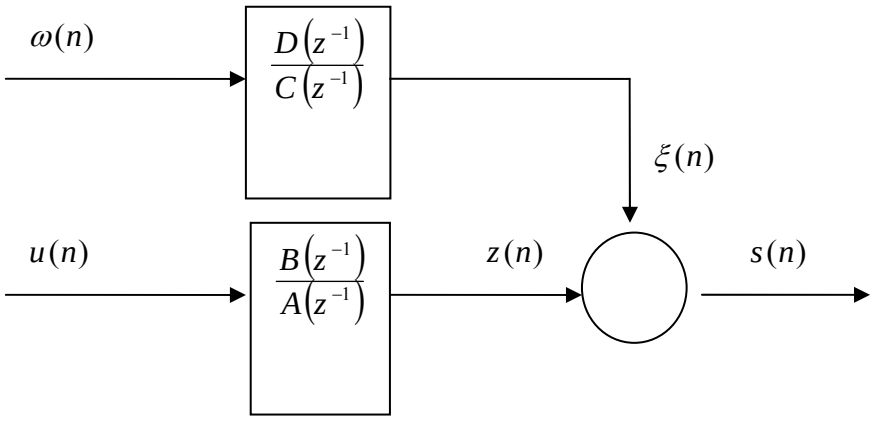

Figure 2.1. Transfer function model of the system

The following ARMAX (autoregressive moving average exogenous variables model) model can be derived from Equation (2.1) and Equation (2.2),

$$s(n) = -\sum_{i=1}^{p} a_i s(n-i) + \sum_{i=0}^{q} b_i u(n-i) + \sum_{i=0}^{l} d_i \omega(n-i) \tag{2.14}$$

By assuming that there is no additive noise equation becomes as follows:

$$s(n) = -\sum_{i=1}^{p} a_i s(n-i) + \sum_{i=0}^{q} b_i u(n-i) \tag{2.15}$$

The autoregressive, AR, model is obtained from Equation (2.11) by assuming b_i=0, 1<i<q and b_0 = K as follows:

$$s(n) = -\sum_{i=1}^{p} a_i s(n-i) + K\,u(n) \tag{2.16}$$

2.2.1.1. AR Parameter Estimation. The system is linear and $s(n)$ is the output of the system where the input is unaccessible. The order of the process, p, and the coefficients a_i, i=1,2,...,p and the gain factor, K, have to be estimated to model the sequence $s(n)$ by AR modeling.

Estimation of the output signal $s(n)$ at time "n" can be described by the following equation,

$$\bar{s}(n) = -\sum_{i=1}^{p} a_i s(n-i) \tag{2.17}$$

Knowing that $\bar{s}(n)$ is the estimated value, error $Err(n)$ in estimation of $\bar{s}(n)$ can be formulised as it is shown below,

$$Err(n) = s(n) - \bar{s}(n) \tag{2.18}$$

$$Err(n) = s(n) + \sum_{i=1}^{p} a_i s(n-i) \tag{2.19}$$

Hence, we can deduce $Err_{expected}$, expected squared error, as,

$$Err_{expected} = E\left\{Err(n)^2\right\} = E\left\{\left[s(n) + \sum_{i=1}^{p} a_i s(n-i) \right]^2 \right\} \tag{2.20}$$

The model coefficients are found as values that minimizes the $Err_{expected}$ satisfying Equation (2.20);

$$\frac{\partial Err_{expected}}{\partial a_m} = 0, \quad 1 \le m \le p \tag{2.21}$$

We can write Equation (2.20) as follows:

$$\sum_{i=1}^{p} a_i E\{s(n-i)s(n-m)\} = -E\{s(n)s(n-m)\} \quad , \quad 1 \le m \le p \tag{2.22}$$

And we can deduce following expression for $Err_{expected}$,

$$Err_{expected} = E\{s^2(n)\} + \sum_{i=1}^{p} a_i E\{s(n-i)s(n-m)\} \tag{2.23}$$

By the stationarity condition of $s(n)$, we can get,

$$E\{s(n-i)s(n-m)\} = R(m-n) \tag{2.24}$$

where $R(m)$ is the autocorrelation function. Equation (2.22) and Equation (2.24) gives us Equation (2.26) known as Yule-Walker or normal equations where

$$R(m-i) = E\{s(n-i)s(n-m)\} = R(i-m) \tag{2.25}$$

$$\sum_{i=1}^{p} a_i R(m-i) = -R(m), \quad 1 \le m \le p \tag{2.26}$$

Here we can see that R, the autocorrelation matrix is symmetric. Then we can express $Err_{expected}$ also as in Equation (2.27)

$$Err_{expected} = R(0) + \sum_{i=1}^{p} a_i R(i) \tag{2.27}$$

The autocorrelation coefficients of the sequence $s(n)$, N being the length of $s(n)$ and n=0,1,...,(N-1), can be estimated as:

$$R(i) = \frac{1}{N} \sum_{n=0}^{N-1-i} s(n)s(n+i) \tag{2.28}$$

Matrix form of Equation (2.26) can be written as

$$\begin{bmatrix} R(0) & R(1) & R(2) & \dots & R(p-1) \\ R(1) & R(0) & R(1) & \dots & R(p-2) \\ R(2) & & & & \\ \vdots & & & & \\ R(p-2) & & \dots & & R(1) \\ R(p-1) & & \dots & & R(0) \end{bmatrix} \begin{bmatrix} a_1 \\ a_2 \\ \\ \\ a_{p-1} \\ a_p \end{bmatrix} = - \begin{bmatrix} R(1) \\ R(2) \\ \\ \\ R(p-1) \\ R(p) \end{bmatrix} \tag{2.29}$$

$$R\underline{a} = -\underline{r} \tag{2.30}$$

Hence AR coefficients can be obtained by the solving Equation (2.30)

$$\underline{a} = -R^{-1}\underline{r} \tag{2.31}$$

A recursive solution of the Equation (2.31) developed by Durbin, gives the AR parameters of order p. Durbin algorithm is given by the following equations,

$$Err_0 = R(0) \tag{2.32}$$

$$t_i = -\frac{\left[R(i) + \sum_{k=1}^{i-1} a_k^{(i-1)} R(i-k)\right]}{Err_{i-1}} \tag{2.33}$$

$$a_i^{(i)} = t_i \tag{2.34}$$

$$a_k^{(i)} = a_k^{(i-1)} + t_i a_{i-k}^{(i-1)} \quad , \quad 1 \le k \le i-1 \tag{2.35}$$

$$Err_i = (1 - t_i^2) Err_{i-1} \quad , \quad 1 \le i \le p \tag{2.36}$$

2.2.2. Power Spectral Density (PSD) Estimation with Welch Periodogram Method

In the Welch method [17] data windows permitting the data segments to overlap in PSD estimation are used. In this method prior to the computation of the segment periodogram a data window is applied to the data. A window provides to reduce the effect of sidelobes and by doing this the effect of estimation bias. Of course this brings a slight decrease in resolution. By overlapping segments the number of segments that are averaged is increased and therefore the PSD estimate variance is decreased.

If we assume s(0), ... , s(N-1) is data record of N samples divided into D segments of L samples each, with a shift of X samples (X<L) , the maximum number of segments D is the integer part of (N-L)/X + 1. The *dth* segment will be as follows,

$$s^{(d)}[n] = w[n]s[n + dX] \tag{2.37}$$

for $0 \le n \le L-1$ and $0 \le d \le D-1$. The spectrum of the *dth* segment is as,

$$\hat{p}_{ss}^{(d)}(f) = \frac{1}{ULT} S^{(d)}(f)\left[S^{(d)}(f)\right]^* = \frac{1}{ULT}\left|S^{(d)}(f)\right|^2 \tag{2.38}$$

where $S^{(d)}(f)$ is the discrete-time Fourier transform of the *dth* segment, U is the discrete

time window energy and the frequence range is $-1/2T \le f \le 1/2T$.

$$S^{(d)}(f) = T\sum_{n=0}^{L-1} s^{d}[n]\exp(-j2\pi fnT) \tag{2.39}$$

$$U = \quad T\sum_{n=0}^{L-1} w^{2}[n] \tag{2.40}$$

Welch periodogram estimate is the average of the windowed segment periodograms and can be expressed as,

$$\hat{p}_{w}(f) = \frac{1}{D}\sum_{d=0}^{D-1} \hat{p}_{ss}^{(d)}(f) \tag{2.41}$$

2.3. Signal Classification and Pattern Recognition

Classification of a signal is associating the signal with the correct class. For this purpose two things are needed: Prior knowledge about classes constituted of pattern vectors representing signals and these pattern vectors to be not redundant. Since samples of signal may contain some redundancies, it is better not to take them directly as pattern vectors. Instead a model that does not contain redundancies is used to represent the signal.

Feature extraction method is one of the efficient method used to model the signal by removing its redundancies. In feature extraction, linear or nonlinear transformations of the original signal is one of the efficient method to represent signal by means of signal features vector. The elements of features vector can be the spectral parameters or the AR parameters of the original measurement. A general pattern classification block diagram is shown in Figure 2.2. Here, classification system produces a single-valued scalar by performing on feature vector. The single-value scalar is the decision, $d_k(\underline{\vartheta})$.

If there are M classes, c_k , $k = 1,2,...,M$, to classify features vector $\underline{\vartheta}$ into one of these classes, M decision functions $d_k(\underline{\vartheta}), k = 1,2,...,M$, should be calculated. The classification is done by comparing M decision functions.

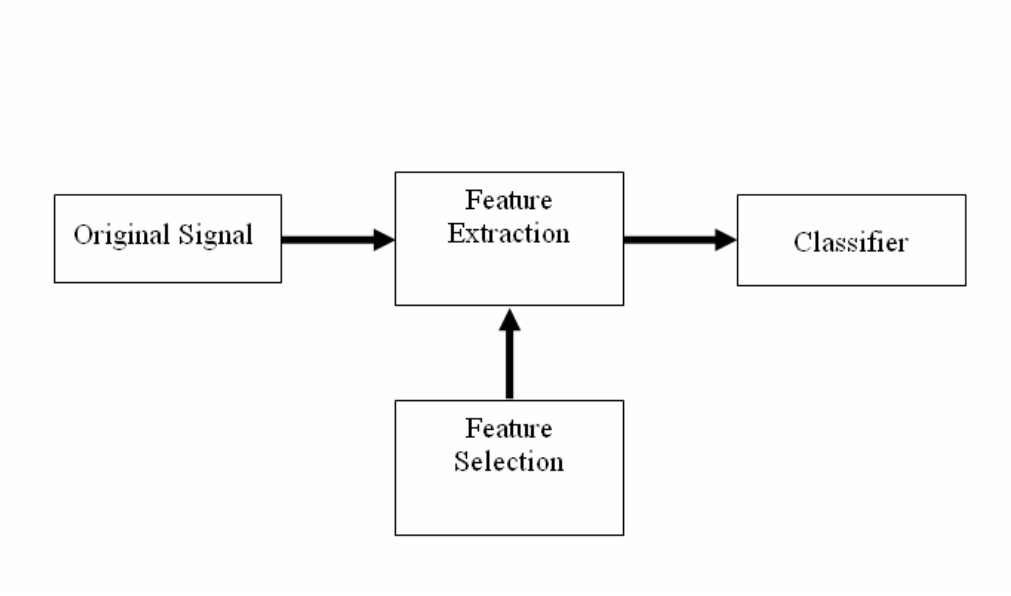

Figure 2.2. Block diagram of pattern classification

In classification a feature vector can be classified in one of the M classes. When classes are well separated from each other, a chosen distance measure can be sufficient to decide that feature vector, $\underline{\vartheta}$, belongs to the class c_k to which $\underline{\vartheta}$ is nearest.

2.3.1. k-Nearest Neighbor (k-NN) Classification

Nearest neighbor (NN) classification method [18] is known especially for well responding in classification problems where boundaries of classes are not separated definitively. The decision about the unknown signal class is done by choosing the class having the nearest neighbor to the signal.

K nearest neighbor classification is another application of the NN classification. In k-NN method, the unknown signal is classified by voting among k nearest neighbor classes

to the signal. The class having maximum number of nearest neighbor is chosen to be the unknown signal class.

The probability of the feature vector $\underline{\vartheta}$ to fall in the sample space R can be described as,

$$P = \int_R p(\underline{\vartheta}) d\vartheta \approx p(\underline{\vartheta})\, V \tag{2.42}$$

with V being the volume of the region R. The approximation in Equation (2.42) is true with the condition that R is small enough. Thus we can write for $p(\underline{\vartheta})$,

$$p(\underline{\vartheta}) = \frac{P}{V} \tag{2.43}$$

If k from n feature vectors constituting the sample space fall in R region then we can deduce that the relationship between P and $p(\underline{\vartheta})$ probabilities is as follows,

$$\hat{P} = \frac{k}{n} \tag{2.44}$$

$$\hat{p}(\underline{\vartheta}) = \frac{k/n}{V} \tag{2.45}$$

The Equation (2.45) necessitates that an appropriate size of V has to be determined. The problem here is that if V is chosen large, the estimation becomes smoother. If V is chosen too small, in this case, the variance of the estimation may increase.

For the two class case, the k-NN classification rule can be sited as,

$$k_1 \succ k_2 \Rightarrow \underline{\vartheta} \in c_1 \tag{2.46}$$

$$k_1 \prec k_2 \Rightarrow \underline{\vartheta} \in c_2 \tag{2.47}$$

The k-NN classification rule for two classes does not require the knowledge about the features statistics.

Leave-one-out method: This method is said to provide good estimates of probability of error in case of small sample populations. In this method, the classifier is trained using all samples except the one to be classified, and then the removed subject is classified.

2.3.2. Distance Measures for k-NN Classifiers

Euclidian distance measure, $D_{Euclidian}$, is one of the distance metrics used for k-NN classification. It is the distance from the class c_k, or from the i^{th} element of the class c_k, $\underline{\vartheta}_{C_k}$, to the feature vector to be classified, $\underline{\vartheta}$.

$D_{Euclidian\ k}$, Euclidian distance of feature vector $\underline{\vartheta}$ to the class c_k, can be expressed as follows :

$$D_{Euclidian\ k}{}^2 = \left\| \underline{\vartheta} - \underline{\vartheta}_{C_k} \right\|^2 = (\underline{\vartheta} - \underline{\vartheta}_{C_k})^T (\underline{\vartheta} - \underline{\vartheta}_{C_k}) \tag{2.48}$$

From Equation (2.48), the decision is that $\underline{\vartheta}$ belongs to the class c_k, if $D_{Euclidian\ k}{}^2$ gives the smallest distance to $\underline{\vartheta}$ in comparison of all $D_{Euclidian}{}^2$ from other classes.

Another distance measure used in classification is Itakura distance [19] measure. Simply, Itakura distance measures the distance between AR models, thus it is used especially when the signal is modeled by using AR models.

The Itakura distance between two AR models, A and B, can be described as in Equation (2.49),

$$d_{Itakura}(A,B) = \log \int_{-\pi}^{\pi} \frac{|A(w)|^2}{|B(w)|^2} \frac{dw}{2\pi} \tag{2.49}$$

The power spectrums of the AR models, $|A(w)|^2$ and $|B(w)|^2$ of models A and B respectively, can be expressed as in Equation (2.50) and Equation (2.51) where a_i and b_i are p^{th} order AR model linear prediction coefficients. Also the gains of the AR models are expressed with σ_A^2 and σ_B^2.

$$|A(w)|^2 = \frac{\sigma_A^2}{\left|1 + a_1 e^{-jw} + ... + a_p e^{-jpw}\right|^2} \tag{2.50}$$

$$|B(w)|^2 = \frac{\sigma_B^2}{\left|1 + b_1 e^{-jw} + ... + b_p e^{-jpw}\right|^2} \tag{2.51}$$

Equation (2.49) can be rewritten by using Equation (2.50) and Equation (2.51) as

$$d_{Itakura}(A,B) = \log \int_{-\pi}^{\pi} \frac{\left|1 + a_1 e^{-jw} + ... + a_p e^{-jpw}\right|^2}{\left|1 + b_1 e^{-jw} + ... + b_p e^{-jpw}\right|^2} \frac{dw}{2\pi} \tag{2.52}$$

We can simplify as

$$d_{Itakura}(A,B) = \log\left(\frac{\underline{b}^T R_A \underline{b}}{\sigma_A^2}\right) \tag{2.53}$$

In Equation (2.53), $\underline{b}^T = [1, b_1, ..., b_p]$ is the AR parameters vector of B, R_A is the autocorrelation vector of model A, σ_A^2 is the gain of model A.

By replacing the autocorrelation matrix R_A with an expression using observation vector $\underline{x}_k$, Equation (2.53) can be transformed into

$$d_{Itakura}(A,B) = \log\left(\frac{\sum_{k=1}^{N} \underline{b}^T \underline{x}_k \underline{x}_k{}^T \underline{b}}{\sum_{k=1}^{N} \underline{a}^T \underline{x}_k \underline{x}_k{}^T \underline{a}}\right) \tag{2.54}$$

where $\underline{x}_k$ is the $(p \times 1)$ observation vector, $\underline{b}^T$ is the reference Linear Predictive Coding (LPC) vector, $\underline{a}^T$ is the LPC vector of the signal to be classified, N is the window length.

Itakura measures the distance by the logarithmic ratio of the squared errors, $Err_A{}^2$ and $Err_B{}^2$, where $Err_A{}^2$ is the error in estimation of the signal to be classified by using the signal's own LPC analysis, and $Err_B{}^2$ is the error in estimation of the same signal by using the reference AR filter parameters. Thus, Equation (2.54) can also be written as,

$$d_{Itakura}(A,B) = \log\left(\frac{\sum_{k=1}^{N} Err_B^2(k)}{\sum_{k=1}^{N} Err_A^2(k)}\right) \tag{2.55}$$

3. METHODOLOGY

3.1. Introduction

27 healthy and 20 pathological subjects were used to record 12 channels of sound data. Informed consent was obtained from the subjects before the recording experiment. The healthy subjects were all nonsmoking adults. Within 37 to 74 age group pathological respiration cycles were selected from subjects consisting of both restrictive and obstructive pulmonary diseases and the pathological lung sounds were heard all over the chest area. Data related to the diseases of the pathological subjects is tabulated in Appendix A.

To record the respiratory sound signals, a multi-channel recording system with 12 channels of sound acquisition and one channel of air-flow measurement has been developed [20]. The sound signals were captured via 12 air-coupled electret microphones (Sony-ECM 44) placed on the posterior chest, with the simultaneous measurement of the air flow using a Fleisch-type flowmeter (Validyne CD 379) for synchronization on the inspiration-expiration cycle. Twelve channels of sound signal were amplified, band-pass filtered between 80-2000 Hz to minimize frictional noise and heart sound interference and to prevent aliasing and digitized by a 12-bit ADC Card (NI-DAQ500) at a 9600 Hz sampling rate to be processed on PC, while flow signal was only low-pass filtered before digitization [21]. Microphone locations are depicted in Figure 3.1 and recordings from 12 microphones are depicted in Figure 3.2.

3.2. Methods Used in the Feature Extraction, Processing and Classification of the Respiratory Sounds

The recorded sound signals were automatically labeled as inspiration and expiration phases based on the flow information. In the analysis and classification of respiratory sounds different feature sets were applied to the k-NN classifier with different distance metrics and their results were compared. In the analysis AR modeling and spectral parameters were used. In classification k-NN classifiers with two different distance metrics, Itakura and Euclidian measures, were applied. Because the sample set was

relatively small, leave-one-out method due to its convenience in case of small sets was applied.

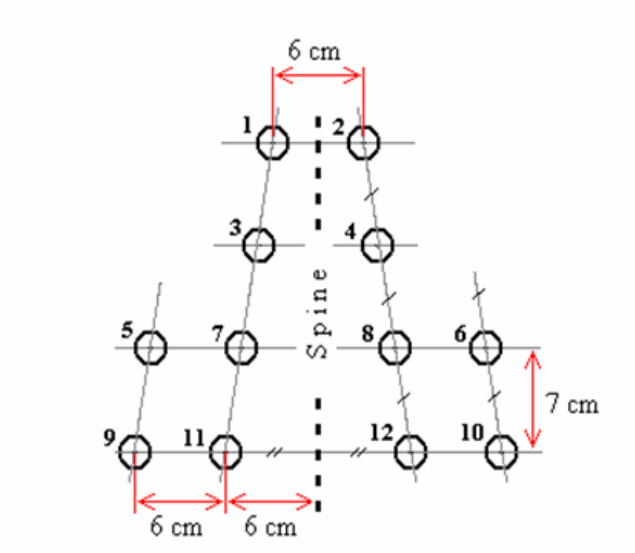

Figure 3.1. Microphone locations on the chest wall

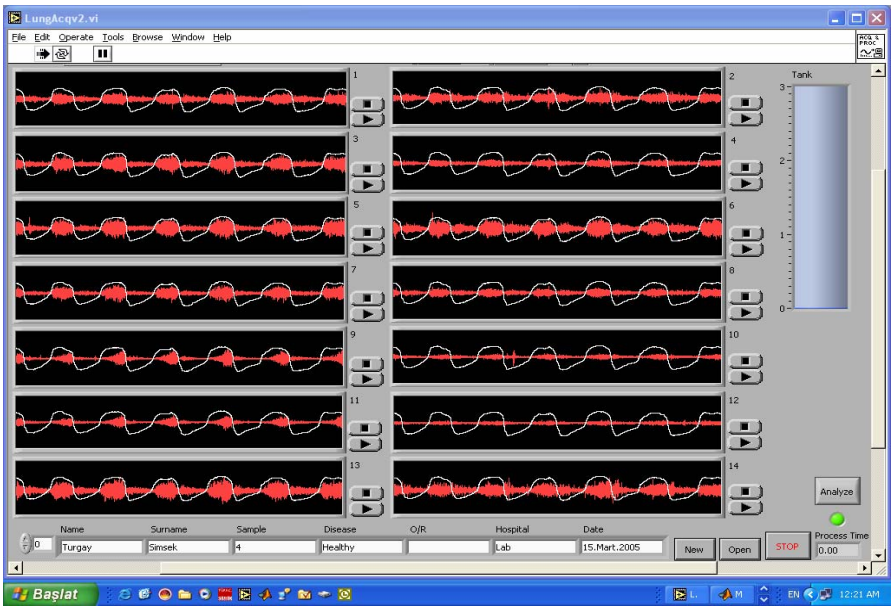

Figure 3.2. 12-channel parallel recordings

All four approaches in feature extraction and classification can be listed as,

- the quantile frequency model with k-NN using Euclidian distance measure, where feature vectors consists of cycle based quantile frequencies.
- the quantile frequency model with k-NN using Euclidian distance measure, where feature vectors consists of segment based quantile frequencies.
- the AR parameter model with k-NN using Euclidian distance measure.
- the AR parameter model with k-NN using Itakura distance measure.

Classification experiments were carried out using k=1, k=3 and k=5 values.

3.2.1. The Cycle Based Quantile Frequency Model

The size of the segments for short-time analysis was chosen to be 512 samples as the respiratory sounds were assumed to be stationary in this interval. Consecutive frames had 25% of overlap. All of the sliding frames were weighted by a Hamming window to reduce the spectral leakage. Thus our sample space consisted of 512 - sample segments of various respiration cycles.

Feature set consisted of quantile frequencies. The power spectral density of all segments were calculated for each channel, for inspiration and expiration cycles separately, and the average of these segment based density functions were taken. From the averaged PSD, the quantile frequencies, namely f25, f50, f75 and f90 were calculated. These percentile frequencies are the frequency points which correspond to the 25%, 50%, 75%, and 90% of the total area under the power spectrum density curve. Thus each channel for each person was represented by one feature vector formed by f25, f50, f75 and f90.

K-NN classifier was chosen for the classification experiment. In the k-NN classification method, the unknown feature vector is classified as belonging to the ith class, if a measure of the distance to its k nearest neighbor in that class is smaller than that of the other class. Euclidean distance metric was used with the classifier and the quantile feature vectors were normalized to equalize the effect of all frequencies before they were inputted to the classifier. Normalization of a vector is done by dividing each element of the vector by the standard deviation of the element after extracting the mean value. Here vector means the data set formed by feature vector elements belonging to the same quantile

frequency group, f25, f50, f75 or f90. Classifiers were trained separately for each channel using the feature space belonging to that channel. Leave-one-out method was employed in performance measurements. This method is said to provide good estimates of probability of error in case of small sample populations. In this method, the classifier is trained using all samples except the one to be classified, and then the removed subject is classified. In the k-NN classifier, k was chosen to be 1, 3 and 5.

The block diagram of respiratory sounds analysis and classification method is given in Figure 3.3.

3.2.2. The Segment Based Quantile Frequency Model

In this model, different from the cycle based quantile frequency model, the feature vector is formed by using quantile frequencies calculated from segment based PSD values. Also in this approach, the PSD of all segments were calculated for each channel and each respiration phases separately. However, instead of taking the average of the PSD of all segments, the quantile frequencies were calculated from PSD of each segment directly. Thus each channel for each person was represented by 30 feature vectors formed by f25, f50, f75 and f90.

Also, to have equal number of feature vectors for each channel and each person, segment number to be used in segmentation was determined apriori. In this case segment number was chosen to be 30, which approximately guarantees segments to be around 512-sample segment.

As in the previous modeling and classification methodology k-NN classifier was chosen for the classification experiment. In the k-NN classification method, Euclidean distance metric was used with the classifier and the percentile feature vectors were normalized to equalize the effect of all frequencies before they were inputed to the classifier. As in the previous method Normalization of a vector is done by dividing each element of the vector by the standard deviation of the element after extracting the mean value. Here vector means the data set formed by feature vector elements belonging to the same quantile frequency group, f25, f50, f75 or f90.

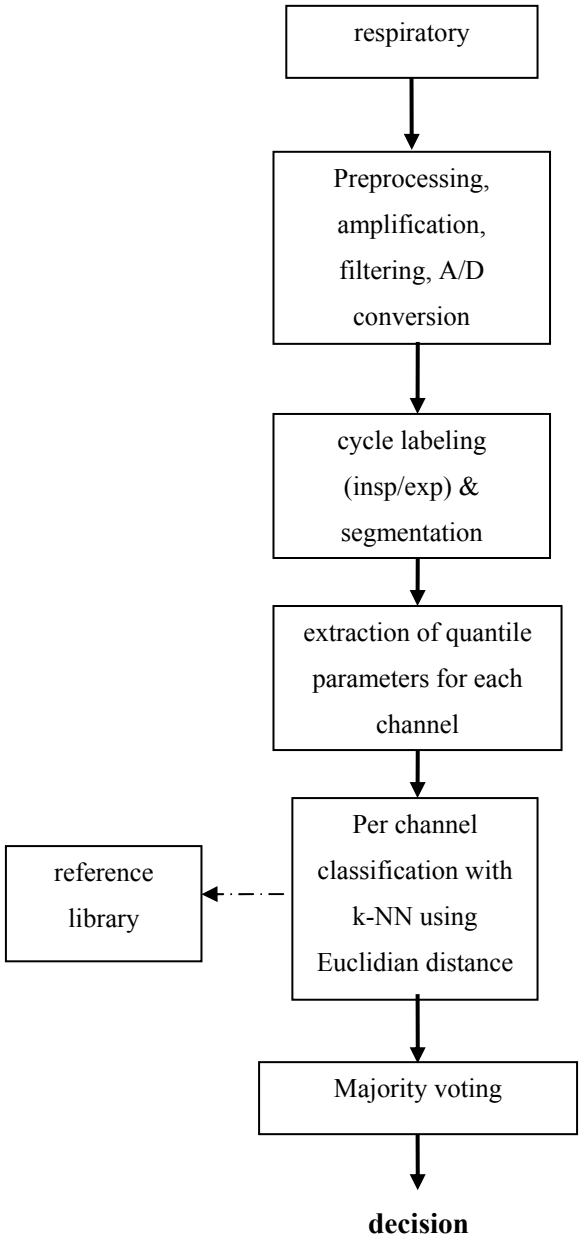

Figure 3.3. Block diagram of k-NN classification using quantile parameters to form feature vectors and Euclidian distance metrics as distance measure

Also in this classification experiment, classifiers were trained separately for each segment of one channel using the feature space belonging to that segment of that channel. Leave-one-out method was employed in performance measurements. In the k-NN classifier, k was chosen to be 1, 3 and 5 in this study.

The block diagram of respiratory sounds analysis and classification method is given in Figure 3.4.

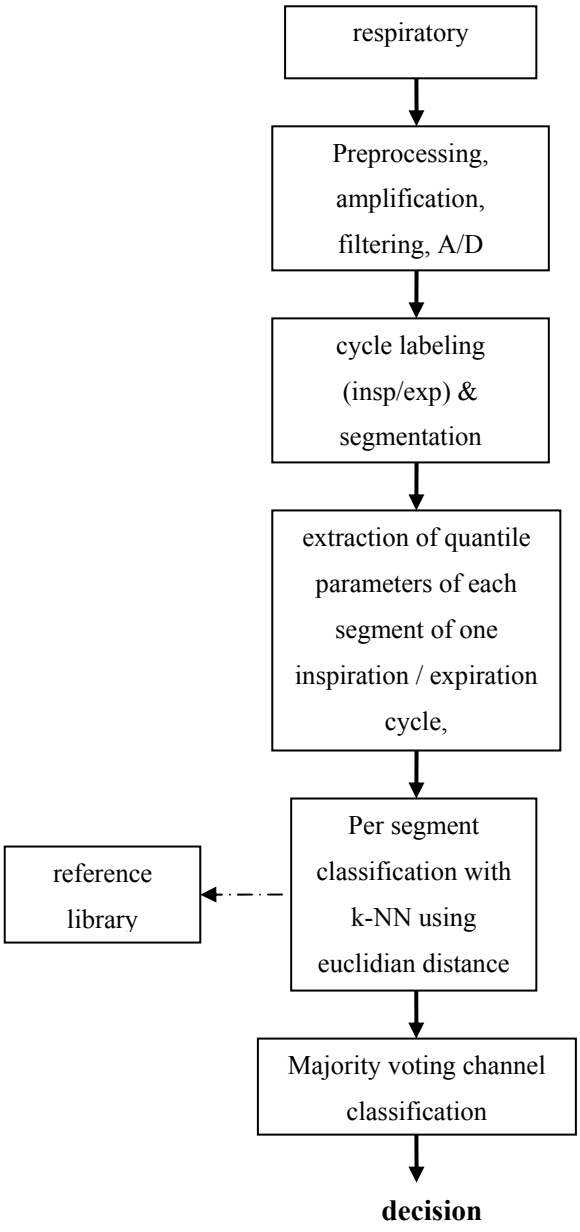

Figure 3.4. Block diagram of k-NN classification using segment based quantile parameters as feature vectors and Euclidian distance metrics as distance measure

3.2.3. AR Parameter Model with k-NN using Euclidian Distance Measure

Feature sets derived from 12 channels of sound data separately for inspiration and expiration cycles were used in the classification experiments. The feature set consisted of AR model coefficients. An autoregressive signal model was assumed for the respiratory sounds. It has been shown in various studies that such a model is suitable for representing lung sound signal [22]. AR parameters were derived for each segment of the respiratory sounds, from the following equation,

$$s_f^{(m)}(n) = \sum_{k=1}^{p} a^{(m)}(k, f)\, s_f^{(m)}(n-k) + e_f^{(m)}(n), n = 1,2,...,N \tag{3.1}$$

where m denotes the segment index, N is the segment size, f labels the inspiration-expiration phases, and a(m) (k,f) is the kth AR coefficient. The segment number is chosen to be 30, which guarantees segments to be approximately 512 - sample segment.

The model order p was chosen to be 6 to establish best order for classification depending on previous researchers reference [20]. Thus each segment of each person is represented by 30 feature vectors formed by 6 AR model coefficients. A multi-channel k-NN classifier with Euclidian distance metric measure was designed. The block diagram of respiratory sounds analysis and classification method is given in Figure 3.5.

3.2.4 AR Parameter Model with k-NN using Itakura Distance Measure

Segmentation is based on a fixed number of segments chosen as 30. Thus each channel of each person is represented by 30 feature vectors formed by 6 AR model coefficients.

All stages of segmentation and feature extraction and feature space formation were same as in the previous method. In classification, a multi-channel k-NN classifier is applied with leave-one-out method but this time Itakura distance measure is chosen as the distance metric.

The block diagram of respiratory sounds analysis and classification method is given in Figure 3.6.

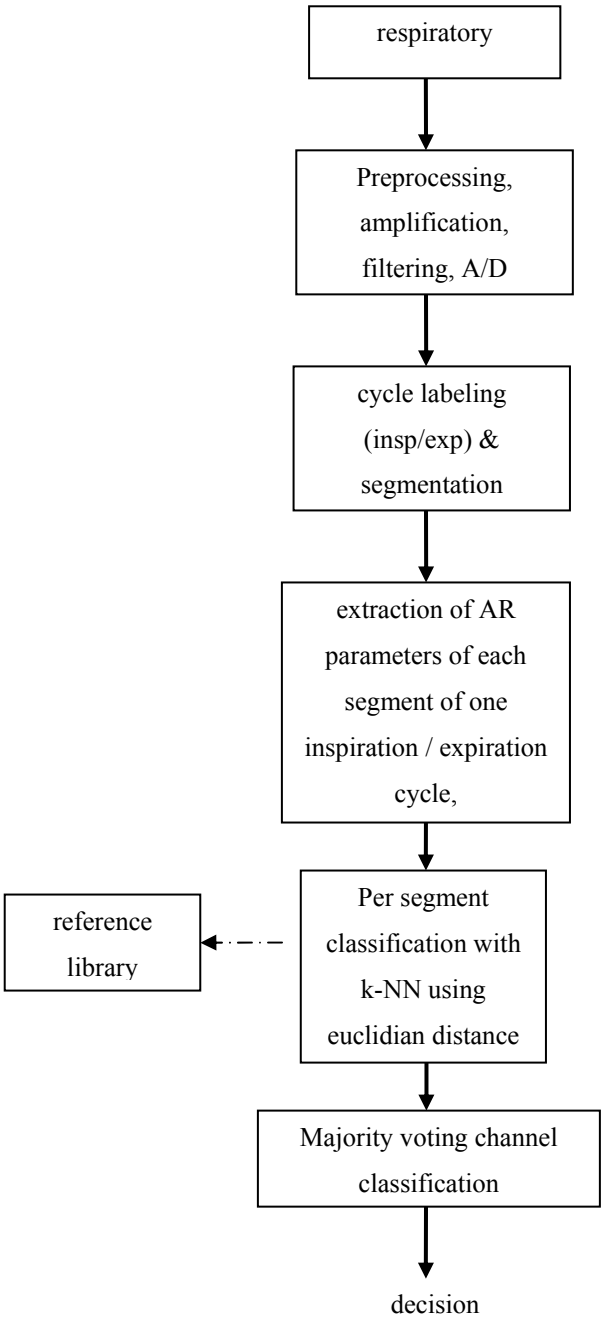

Figure 3.5. Block diagram of k-NN classification using AR parameters as feature vectors and Euclidian distance metrics as distance measure

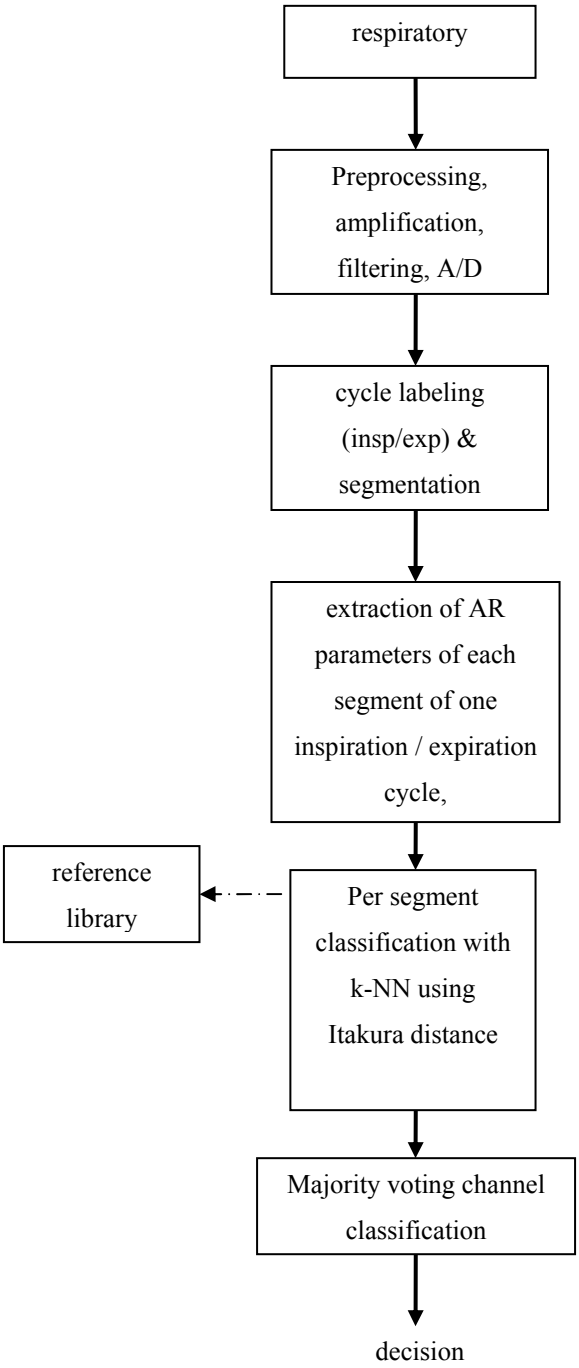

Figure 3.6. Block diagram of k-NN classification using AR parameters as feature vectors and Itakura distance metrics as distance measure

3.3. Experimental Results

As mentioned before 12-channel sound data recorded from 27 healthy and 20 pathological subjects were used. The healthy subjects were all nonsmoking adults.

Pathological respiration cycles were selected from subjects consisting of both restrictive and obstructive pulmonary diseases and the pathological lung sounds were heard all over the chest area. The recorded sound signals were processed differently depending on all four classification methodologies explained in previous section.

Figure 3.7 and Figure 3.8 display respiratory sounds in pathological and healthy cases and their flow signals, respectively. Figure 3.9 to Figure 3.20 consist of PSD functions calculated as the average of 27 subjects for healthy and 20 subjects for pathological group for each channel in expiration respiratory phase. Figure 3.21 to Figure 3.32 are average PSD of each channel for inspiration. It can be observed that in both phases, average PSD curves of pathological subjects reach higher frequencies than healthy subjects.

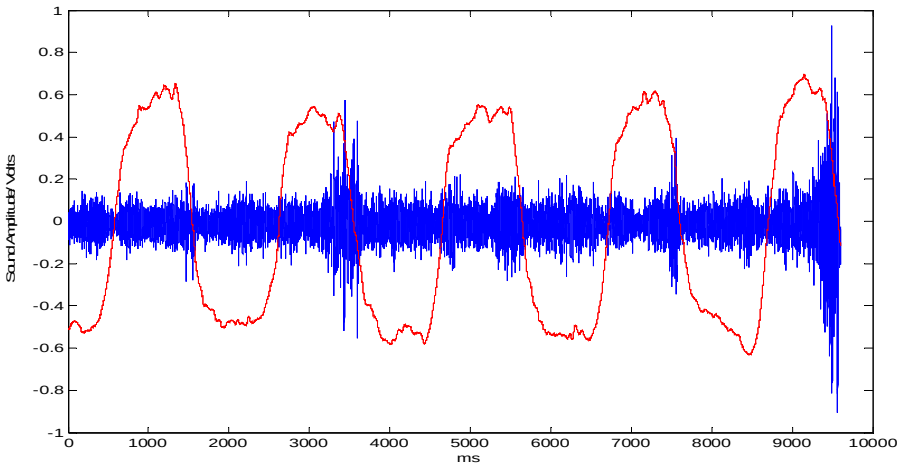

Figure 3.7. Respiratory sound and flow sample of a healthy subject

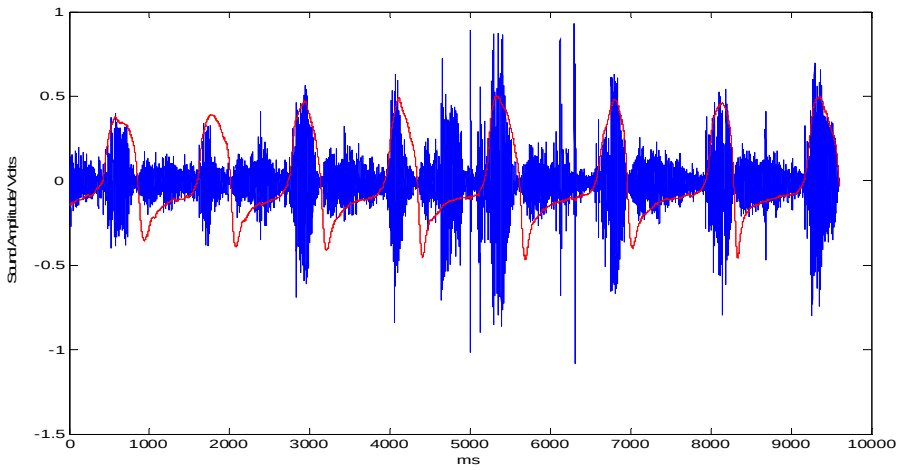

Figure 3.8. Respiratory sound and flow sample of a pathological subject

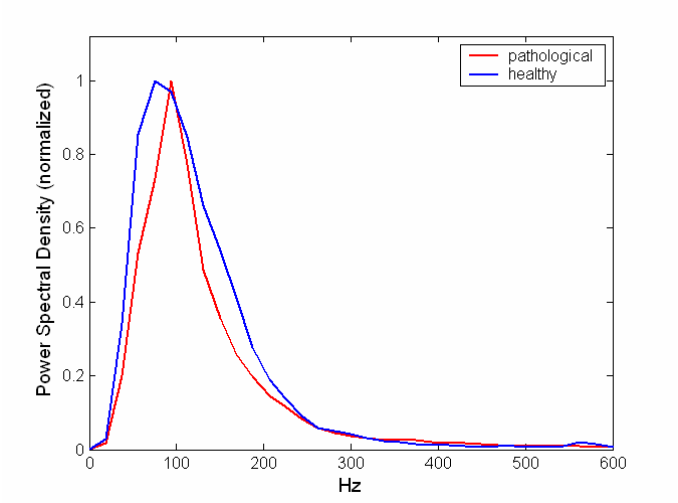

Figure 3.9. Average PSD of 20 pathological and 27 healthy subjects for expiration phase for channel 1

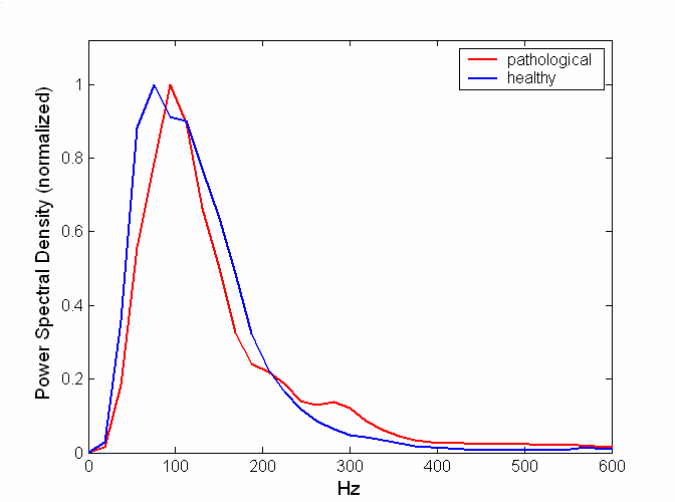

Figure 3.10. Average PSD of 20 pathological and 27 healthy subjects for expiration phase for channel 2

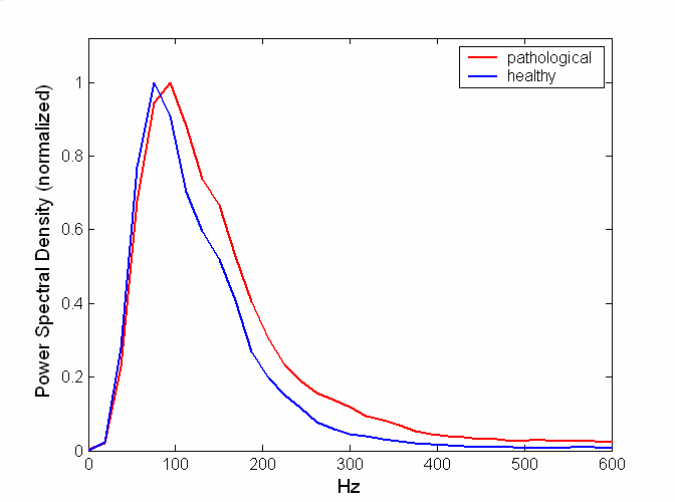

Figure 3.11. Average PSD of 20 pathological and 27 healthy subjects for expiration phase for channel 3

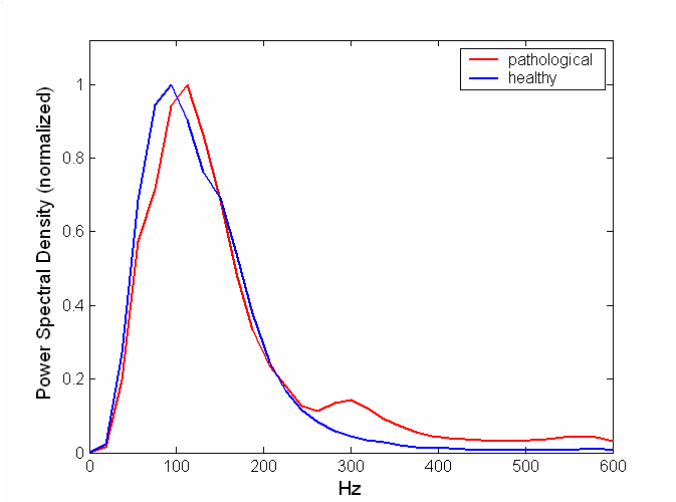

Figure 3.12. Average PSD of 20 pathological and 27 healthy subjects for expiration phase for channel 4

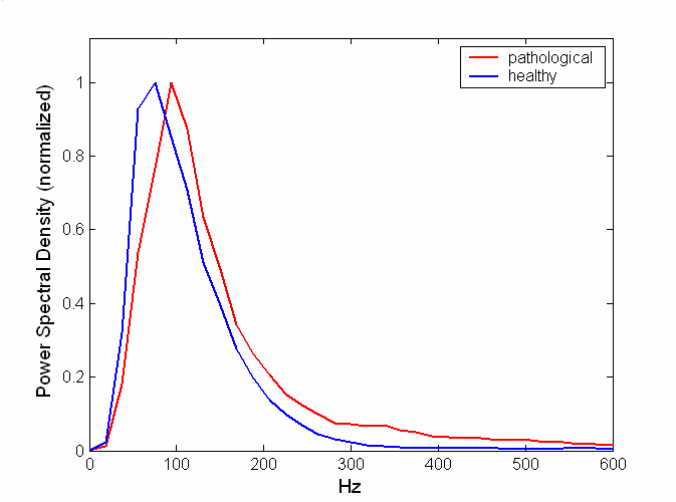

Figure 3.13. Average PSD of 20 pathological and 27 healthy subjects for expiration phase for channel 5

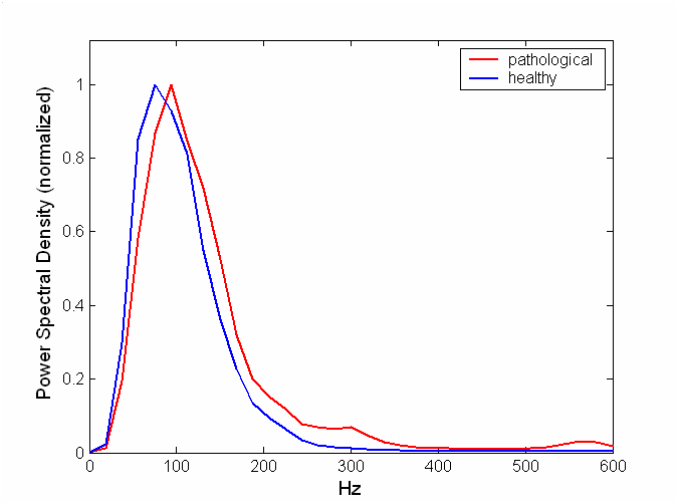

Figure 3.14. Average PSD of 20 pathological and 27 healthy subjects for expiration phase for channel 6

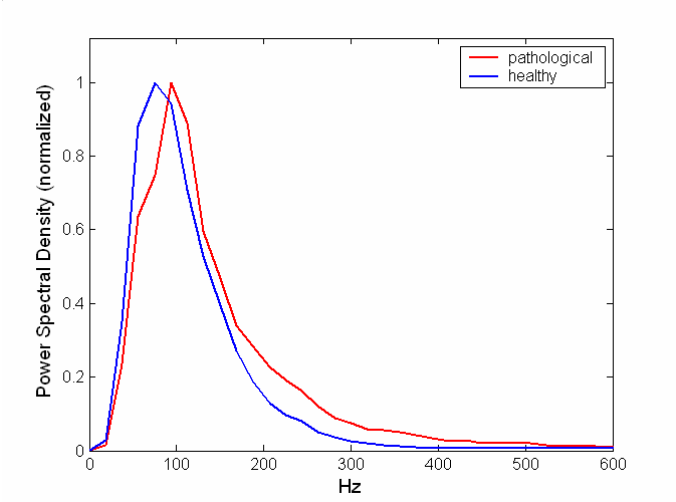

Figure 3.15. Average PSD of 20 pathological and 27 healthy subjects for expiration phase for channel 7

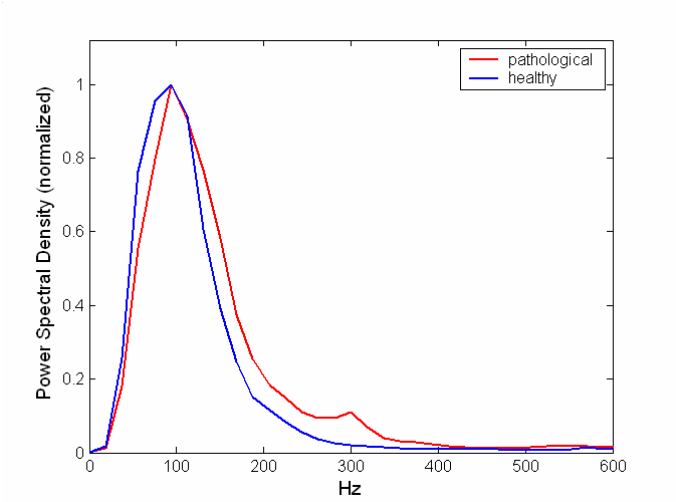

Figure 3.16. Average PSD of 20 pathological and 27 healthy subjects for expiration phase for channel 8

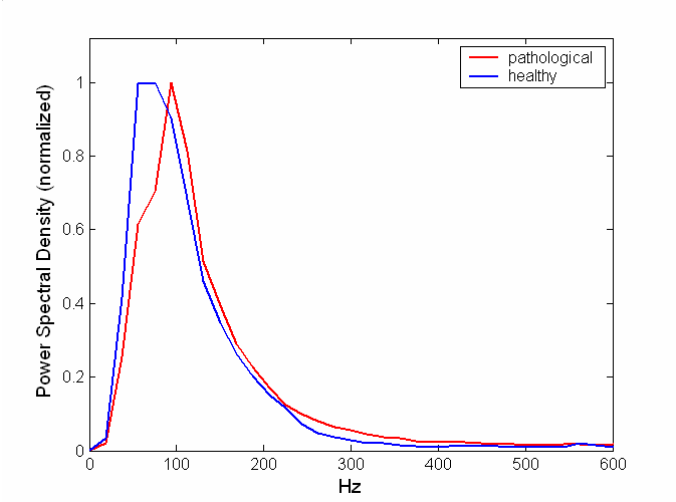

Figure 3.17. Average PSD of 20 pathological and 27 healthy subjects for expiration phase for channel 9

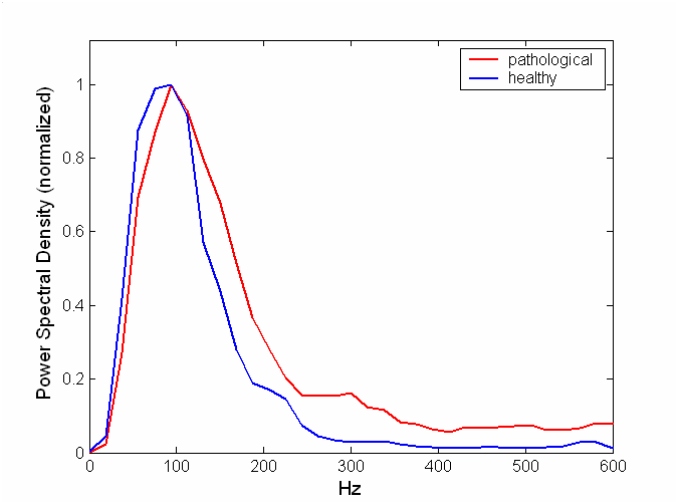

Figure 3.18. Average PSD of 20 pathological and 27 healthy subjects for expiration phase for channel 10

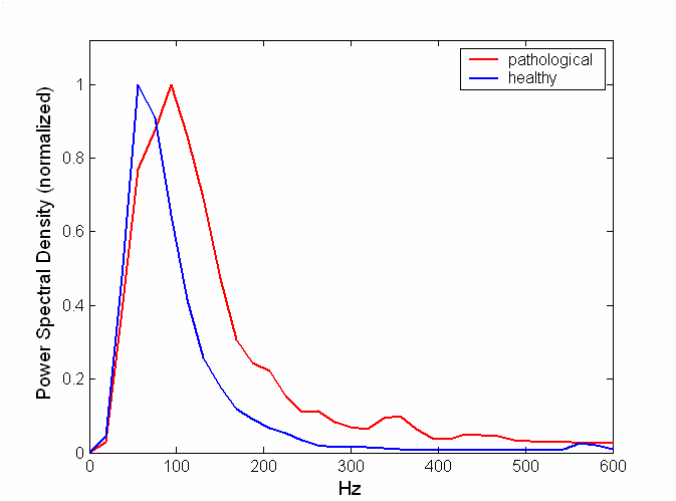

Figure 3.19. Average PSD of 20 pathological and 27 healthy subjects for expiration phase for channel 11

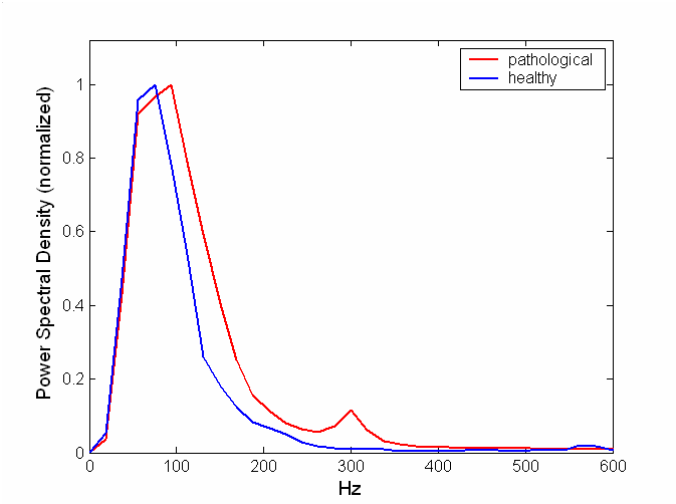

Figure 3.20. Average PSD of 20 pathological and 27 healthy subjects for expiration phase for channel 12

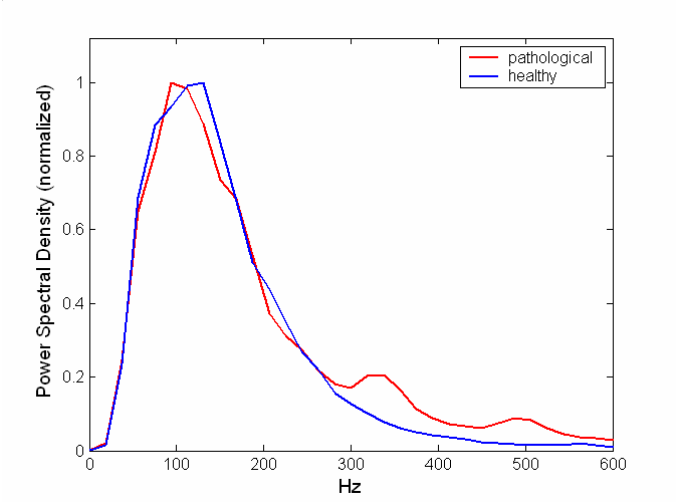

Figure 3.21. Average PSD of 20 pathological and 27 healthy subjects for inspiration phase for channel 1

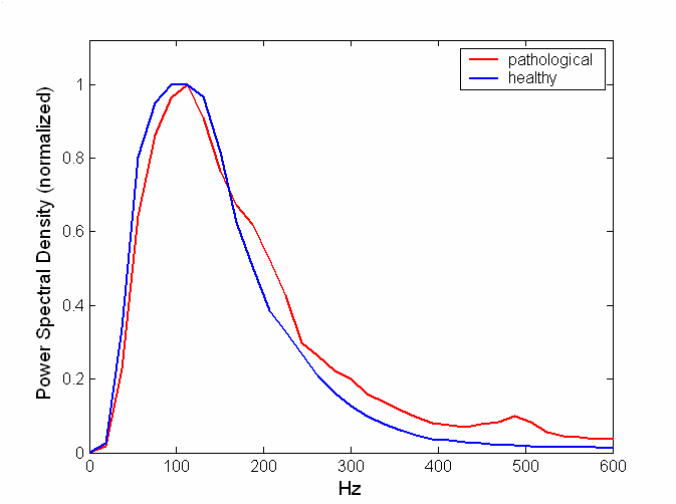

Figure 3.22. Average PSD of 20 pathological and 27 healthy subjects for inspiration phase for channel 2

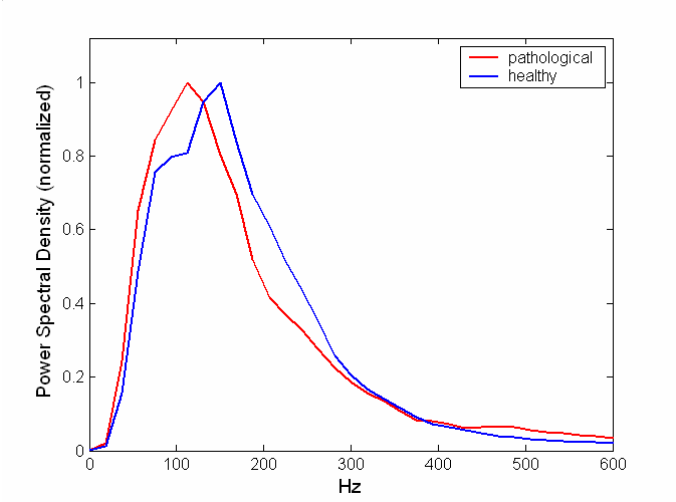

Figure 3.23. Average PSD of 20 pathological and 27 healthy subjects for inspiration phase for channel 3

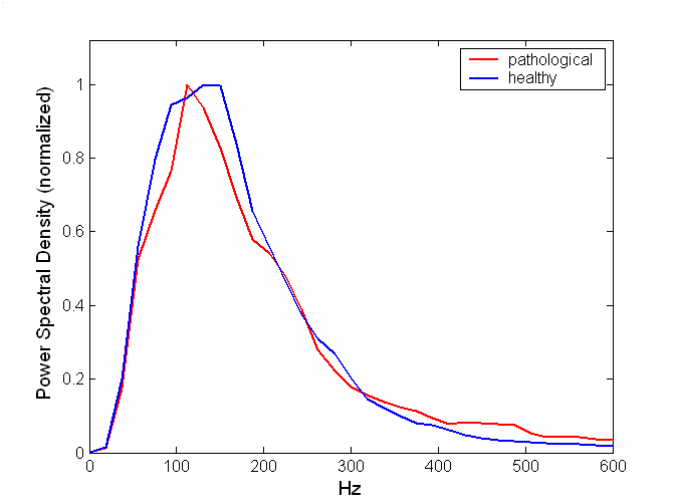

Figure 3.24. Average PSD of 20 pathological and 27 healthy subjects for inspiration phase for channel 4

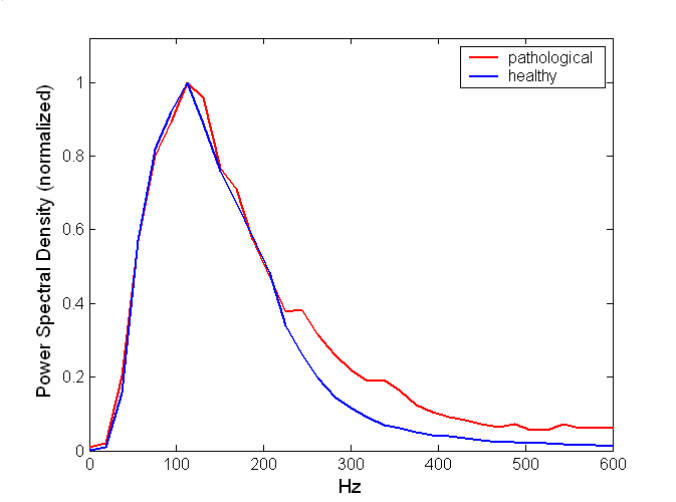

Figure 3.25. Average PSD of 20 pathological and 27 healthy subjects for inspiration phase for channel 5

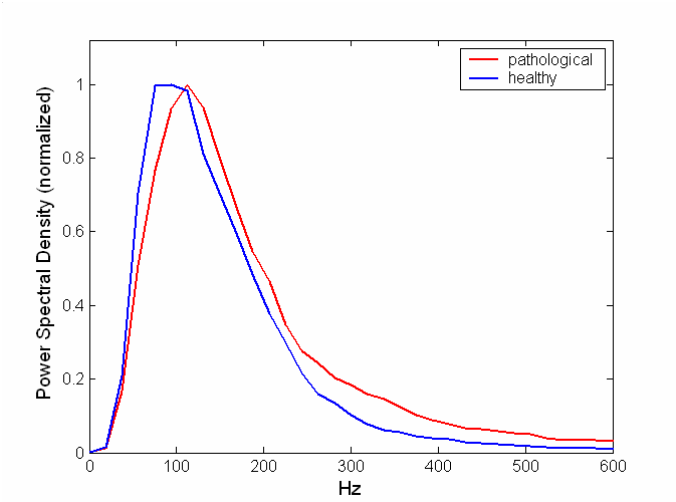

Figure 3.26. Average PSD of 20 pathological and 27 healthy subjects for inspiration phase for channel 6

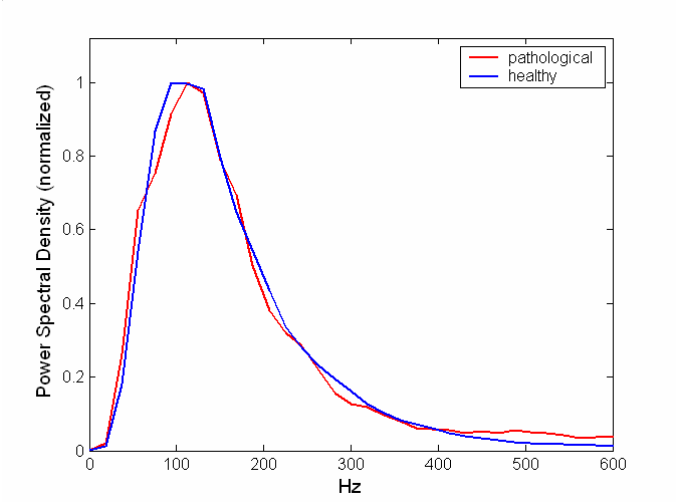

Figure 3.27. Average PSD of 20 pathological and 27 healthy subjects for inspiration phase for channel 7

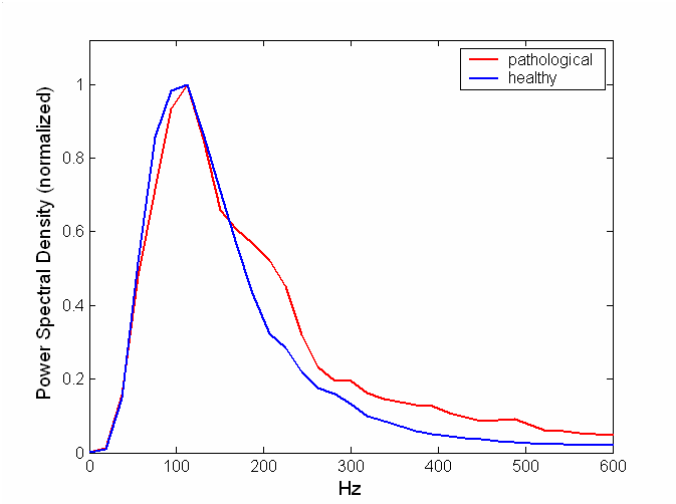

Figure 3.28. Average PSD of 20 pathological and 27 healthy subjects for inspiration phase for channel 8

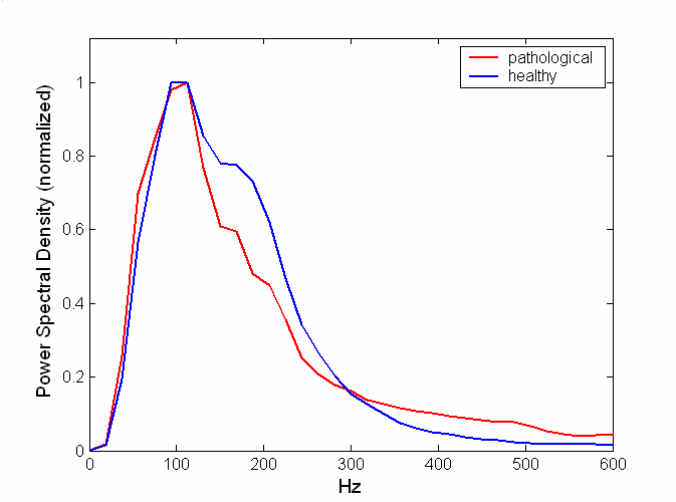

Figure 3.29. Average PSD of 20 pathological and 27 healthy subjects for inspiration phase for channel 9

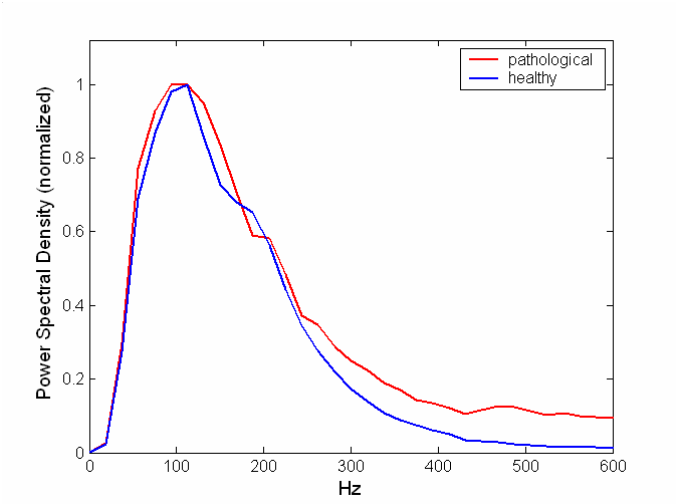

Figure 3.30. Average PSD of 20 pathological and 27 healthy subjects for inspiration phase for channel 10

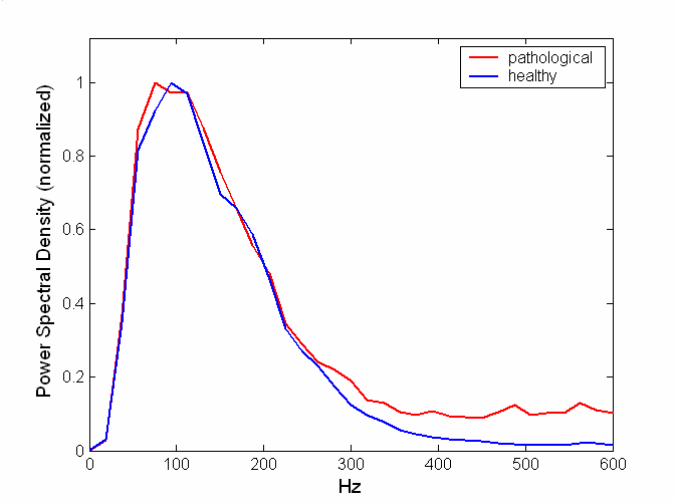

Figure 3.31. Average PSD of 20 pathological and 27 healthy subjects for inspiration phase for channel 11

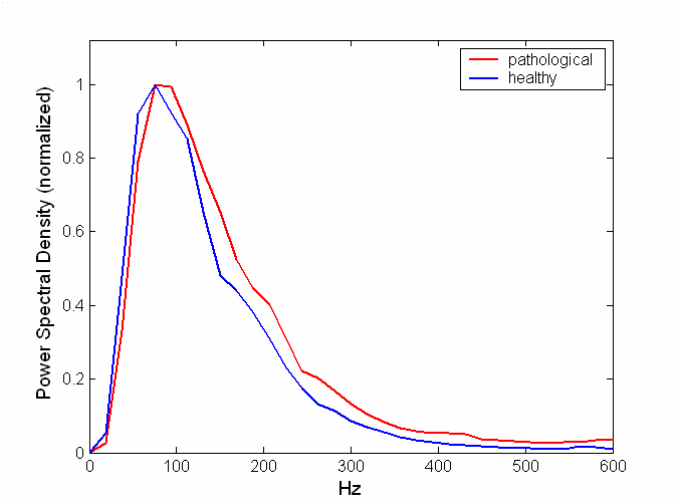

Figure 3.32. Average PSD of 20 pathological and 27 healthy subjects for inspiration phase for channel 12

Averaged PSD were calculated for each channel (average PSD values of 27 healthy and 20 pathological subjects). Figure 3.33 to Figure 3.44 depict these curves for different channel groups. Channel groups are chosen as (i) channels 2, 4, 8, 12, (ii) channels 1, 3, 7, 11 and (iii) channels 5, 7, 8, 6, corresponding to two vertical and one horizontal scan, respectively.

For each group four figures consisting of inspiration, expiration phases of healthy and pathological cases exist. In figures instead of comparing healthy and pathological cases, the frequency differentiation via channels in subjects is aimed to be displayed. As a result, it can be seen that in especially healthy subjects the frequency characteristics of the respiratory sound differ depending on microphone location. This is seen especially in figures for two vertical scan group, 2,4,8,12 and 1,3,7,11, in healthy case for both, inspiration and expiration phases clearly. Thus, in classification, the consideration of microphone locations is expected to give more accurate results about the subject class.

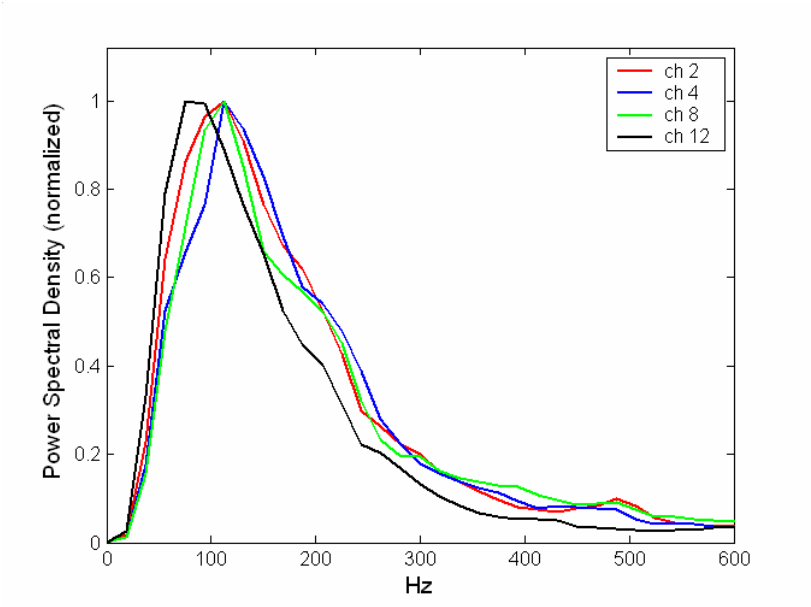

Figure 3.33. Average PSD of 20 pathological subjects for inspiration phase for channels 2,4,8,12

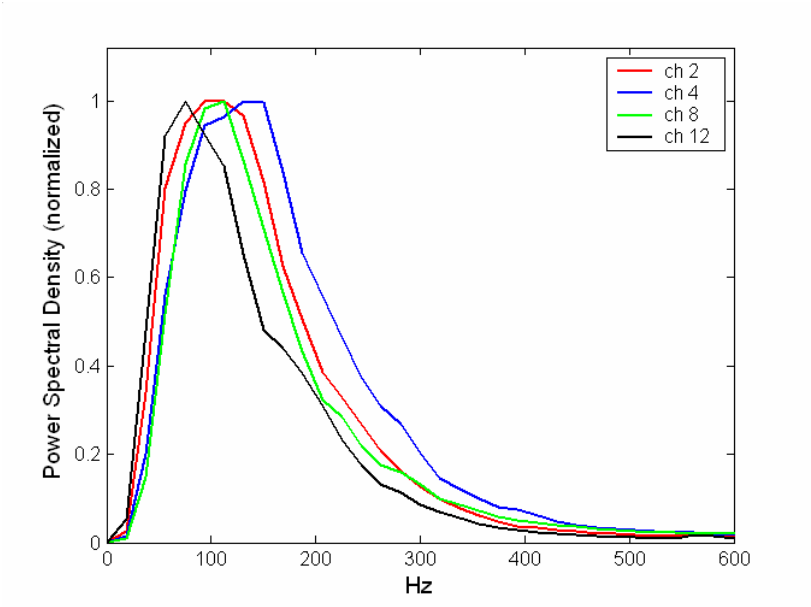

Figure 3.34. Average PSD of 27 healthy subjects for inspiration phase for channels 2,4,8,12

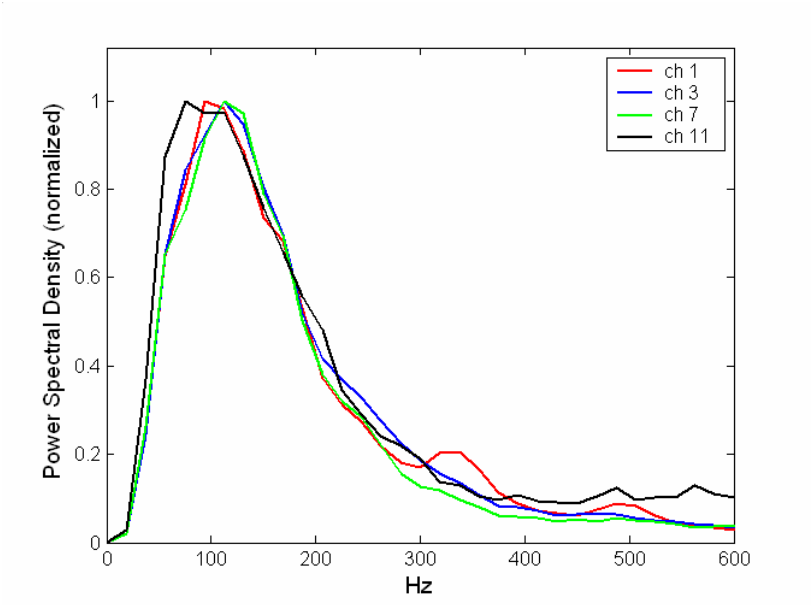

Figure 3.35. Average PSD of 20 pathological subjects for inspiration phase for channels 1,3,7,11

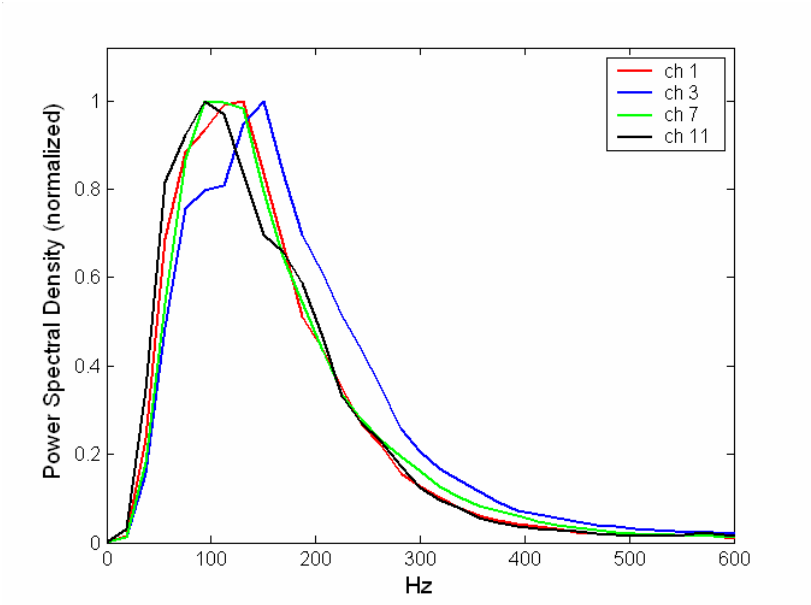

Figure 3.36. Average PSD of 27 healthy subjects for inspiration phase for channels 1,3,7,11

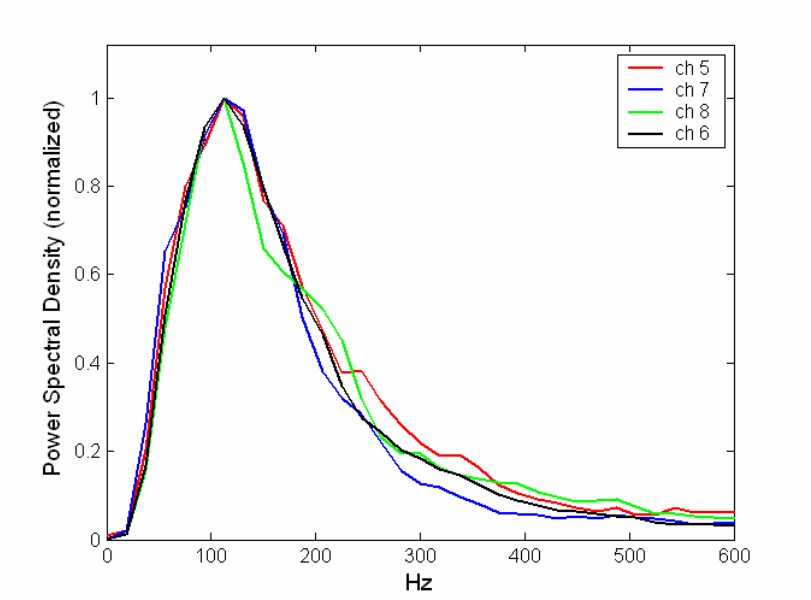

Figure 3.37. Average PSD of 20 pathological subjects for inspiration phase for channels 5,7,8,6

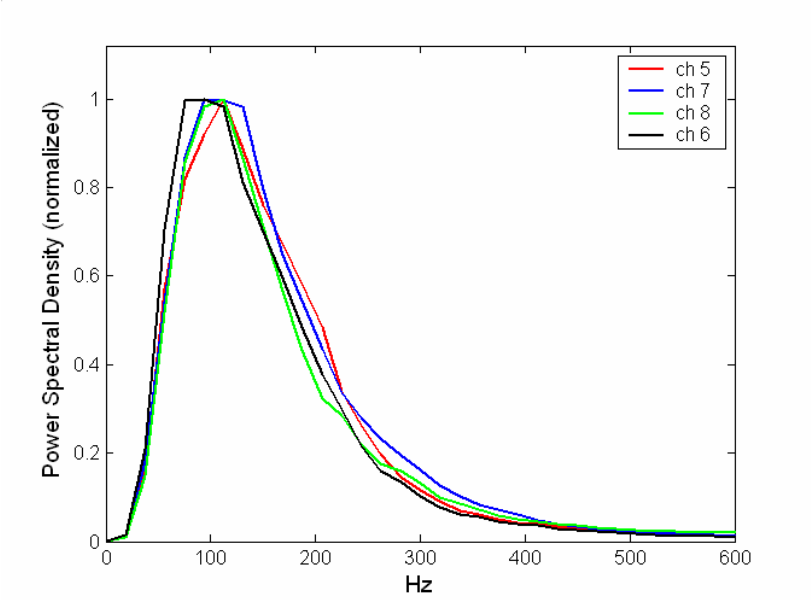

Figure 3.38. Average PSD of 27 healthy subjects for inspiration phase for channels 5,7,8,6

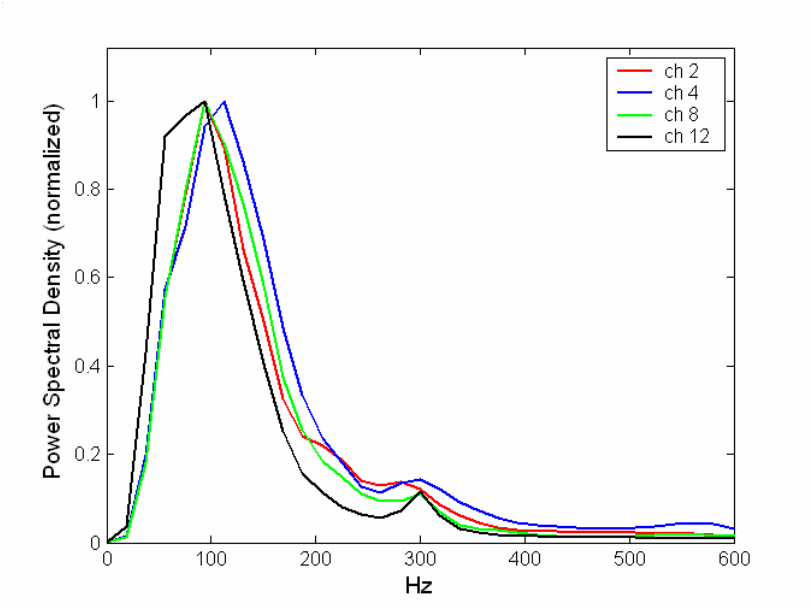

Figure 3.39. Average PSD of 20 pathological subjects for expiration phase for channels 2,4,8,12

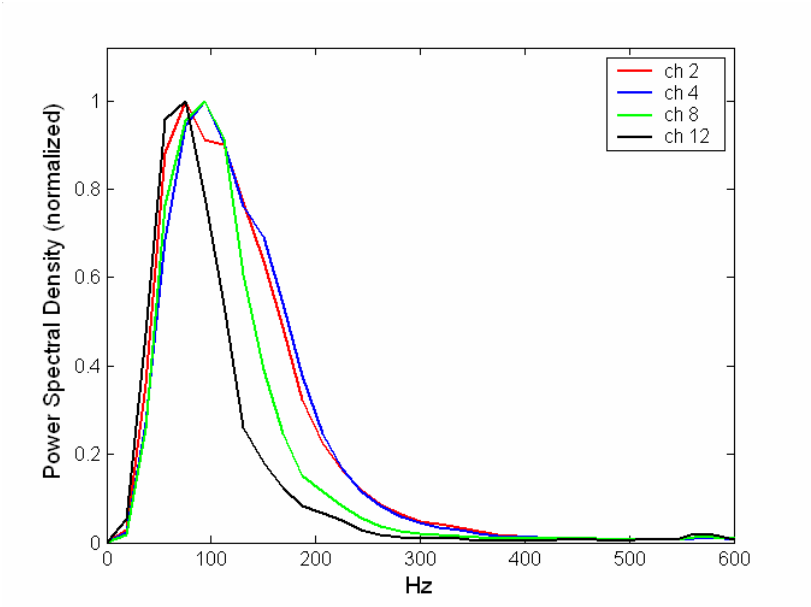

Figure 3.40. Average PSD of 27 healthy subjects for expiration phase for channels 2,4,8,12

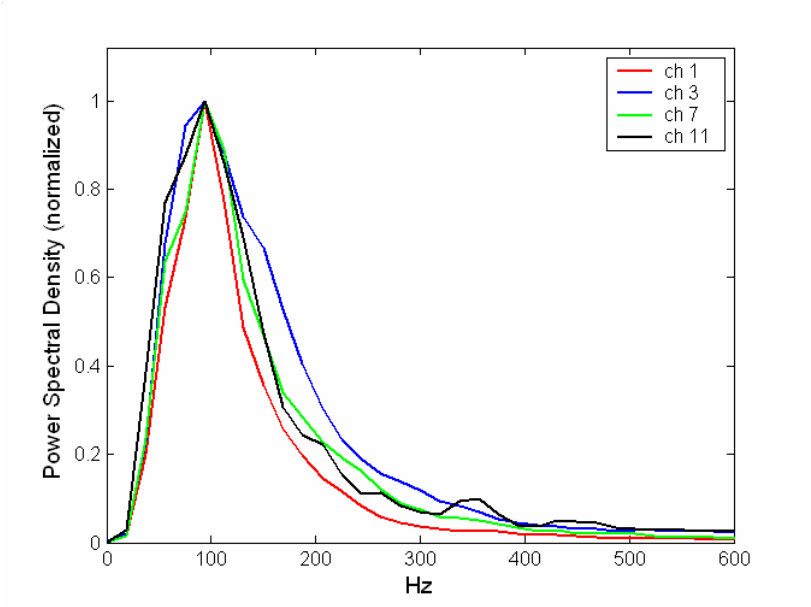

Figure 3.41. Average PSD of 20 pathological subjects for expiration phase for channels 1,3,7,11

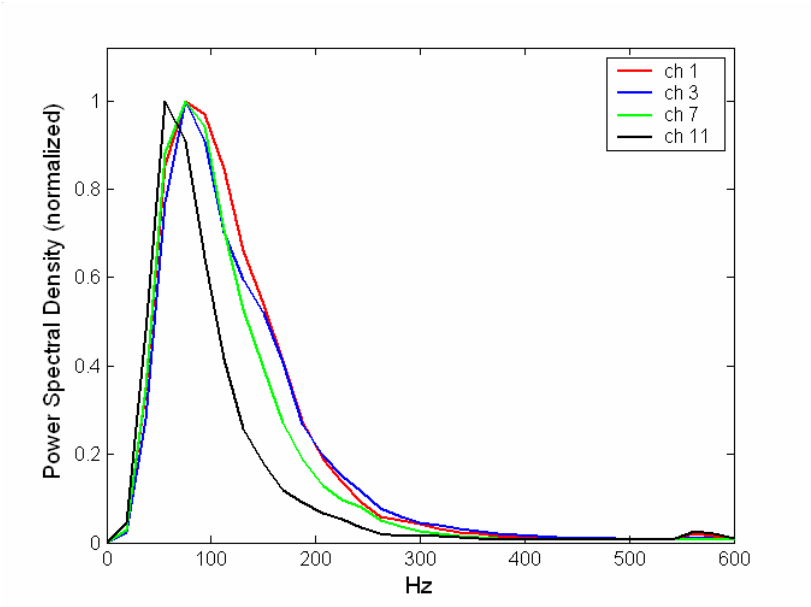

Figure 3.42. Average PSD of 27 healthy subjects for expiration phase for channels 1,3,7,11

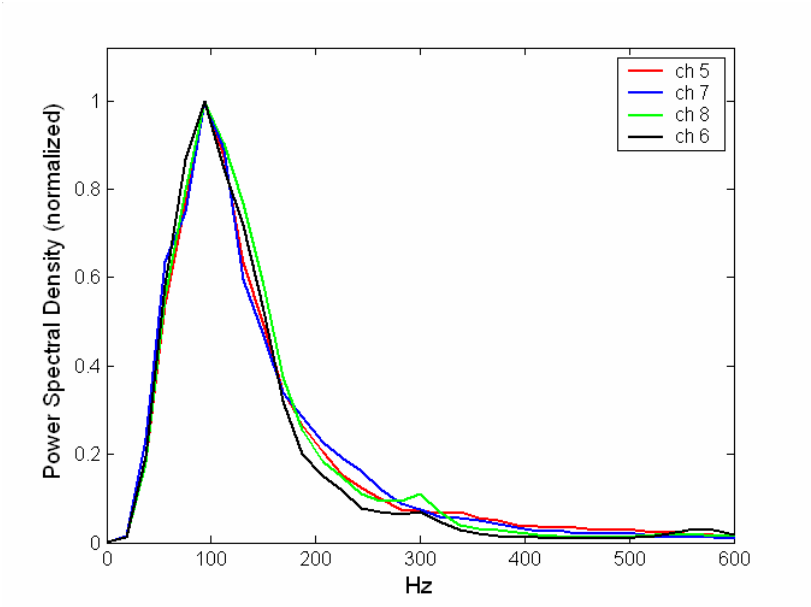

Figure 3.43. Average PSD of 20 pathological subjects for expiration phase for channels 5,7,8,6

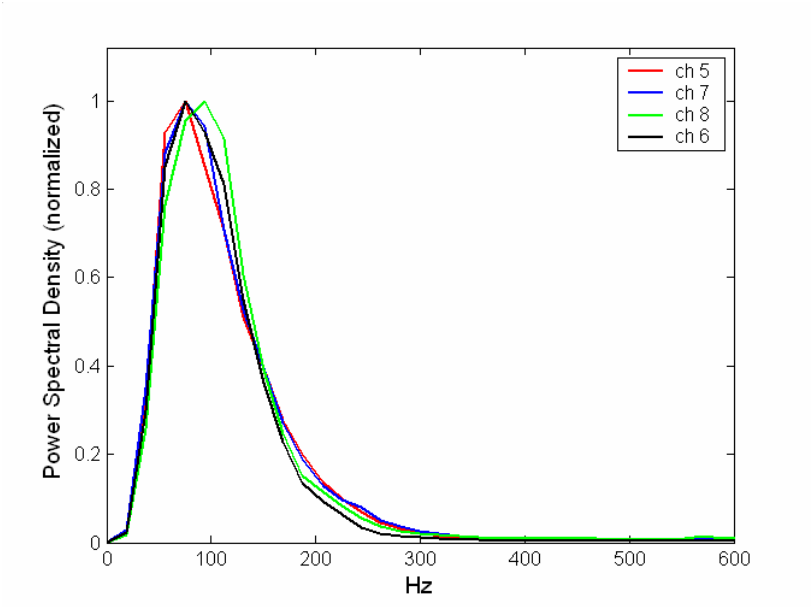

Figure 3.44. Average PSD of 27 healthy subjects for expiration phase for channels 5,7,8,6

Also for each channel, quantile frequency values, f25, f50, f75 and f90, were calculated for each respiration phase, inspiration and expiration, separately. The average (average value of 20 pathological and 27 healthy subjects), maximum and minimum

frequency related to each quantile frequency are displayed. Healthy and pathological cases are depicted together. In figures quantile frequency values over 500Hz are not displayed. These are shown in Figure 3.45 to Figure 3.52. Generally in pathological subjects for any quantile frequency value, average frequency values were observed to be higher than that of healthy subjects.

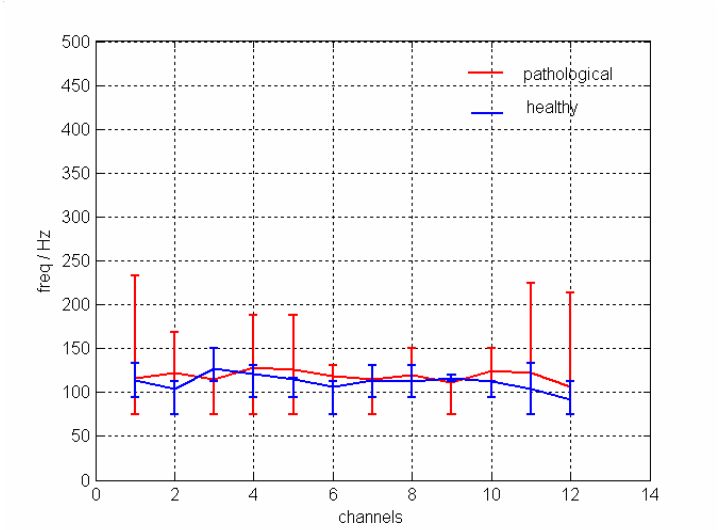

Figure 3.45. Averaged quantile frequency (25%) of 47 subjects for each channel for inspiration phase

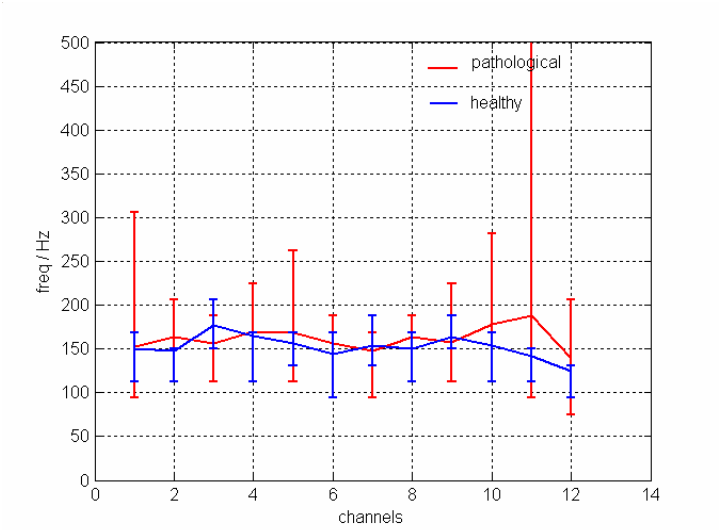

Figure 3.46. Averaged quantile frequency (%50) of 47 subjects for each channel for inspiration phase

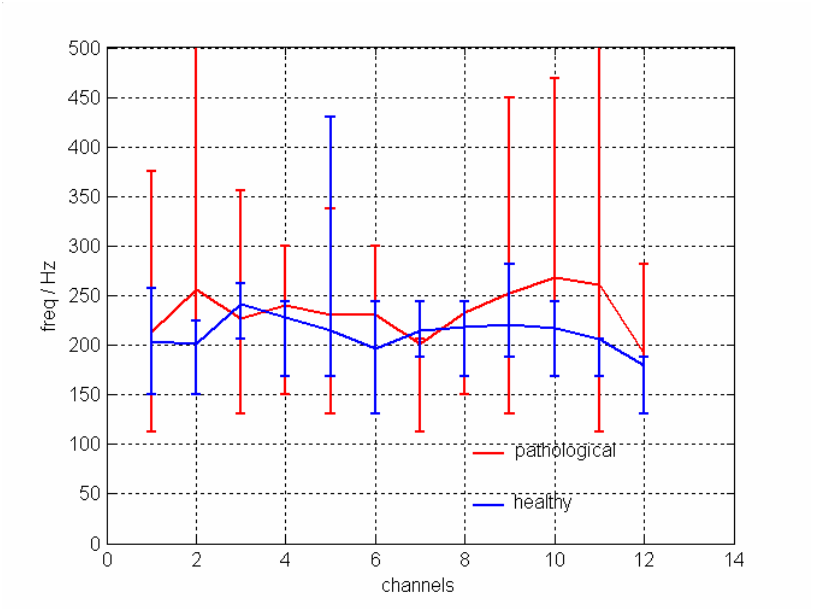

Figure 3.47. Averaged quantile frequency (75%) of 47 subjects for each channel for inspiration phase

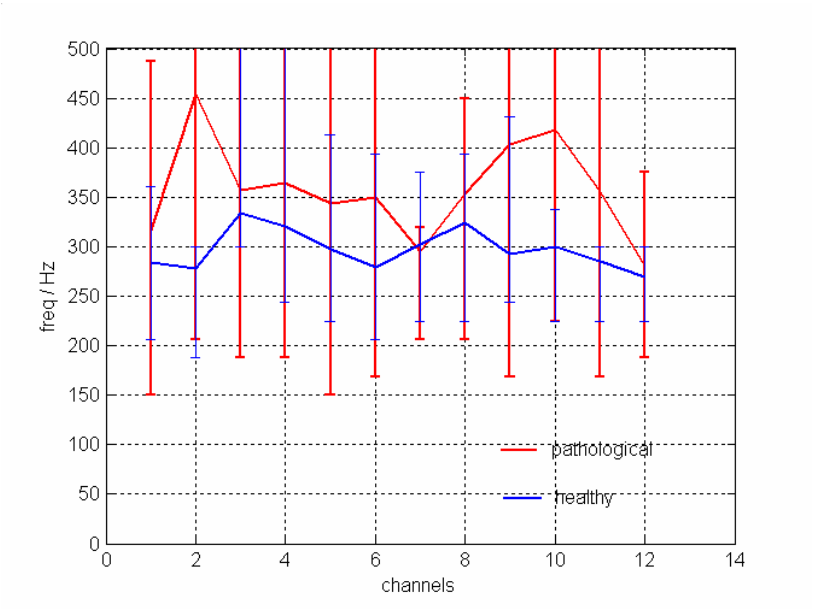

Figure 3.48. Averaged quantile frequency (90%) of 47 subjects for each channel for inspiration phase

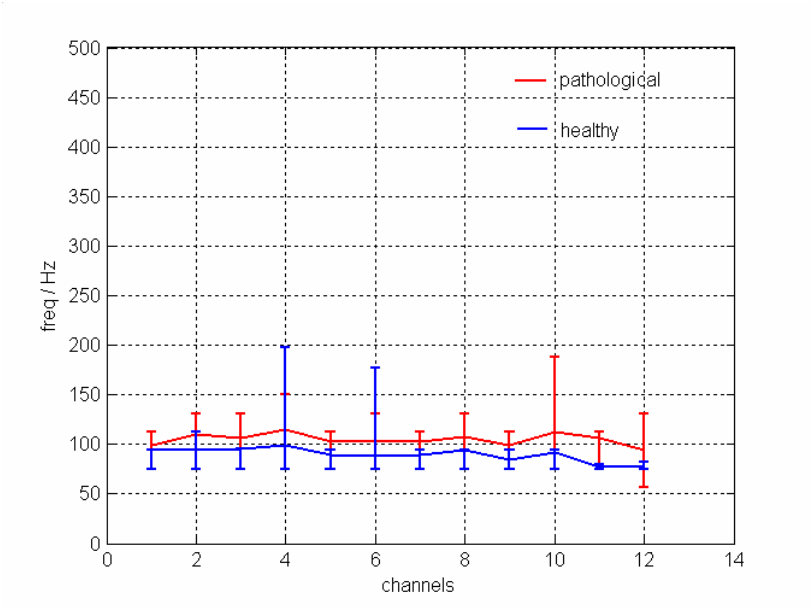

Figure 3.49. Averaged quantile frequency (25%) of 47 subjects for each channel for expiration phase

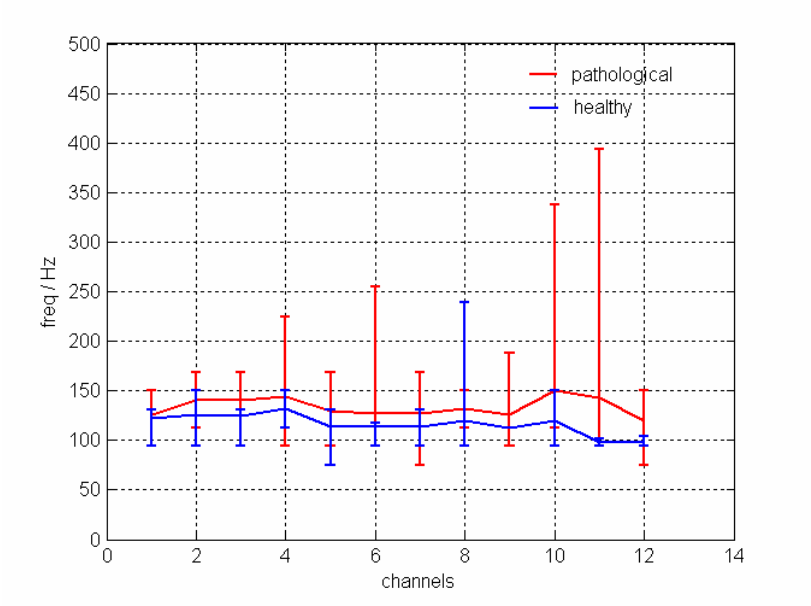

Figure 3.50. Averaged quantile frequency (50%) of 47 subjects for each channel for expiration phase

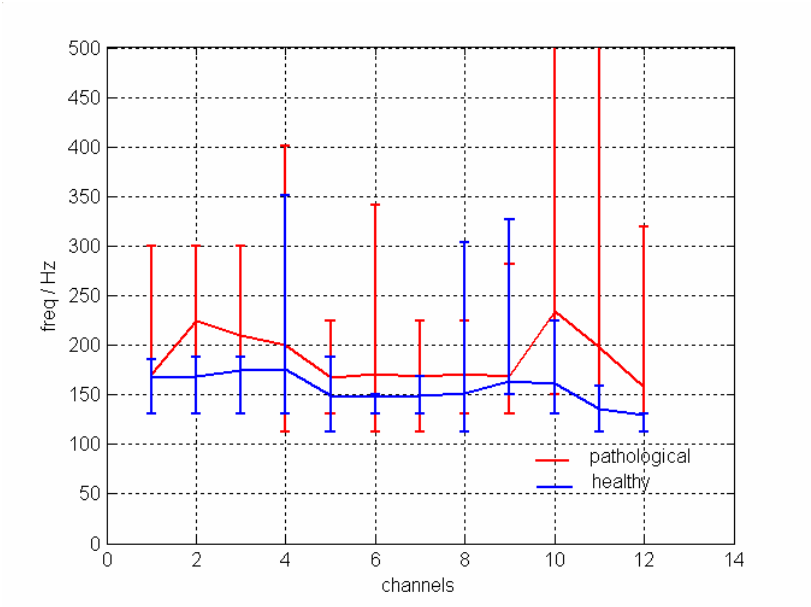

Figure 3.51. Averaged quantile frequency (75%) of 47 subjects for each channel for expiration phase

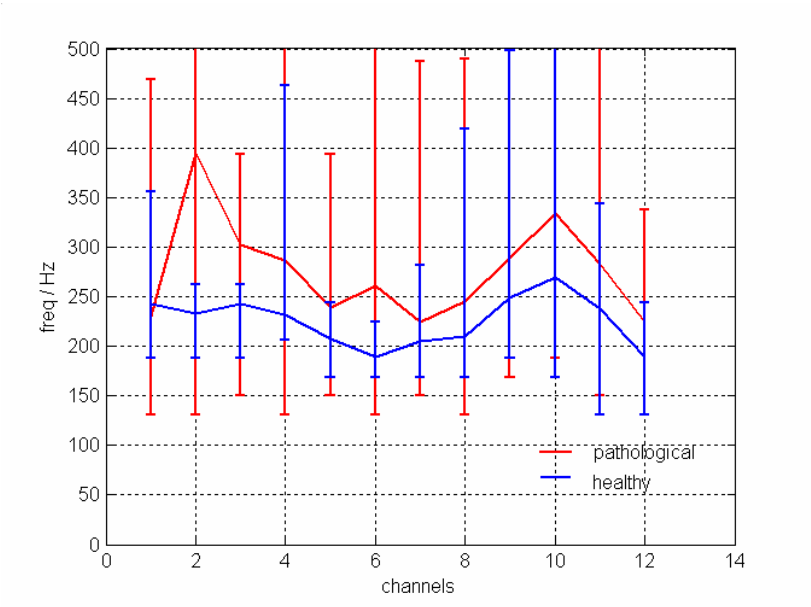

Figure 3.52. Averaged quantile frequency (90%) of 47 subjects for each channel for expiration phase

3.4. Performance Criteria and Results Comparison

Four different methods of analysis and classification were performed on 27 healthy and 20 pathological respiration cycles. The cycles were recorded via 12 microphones placed on the posterior chest.

Different methodologies of classification were performed. In section 3 methodologies are explained in detail. Performance of the classifiers was measured and compared. Measurement metrics were chosen as sensitivity, $S\%$, specificity, $SP\%$, and accuracy, $CC\%$. These values are given by the following equations:

$$S\% = \frac{T_{pathological}}{T_{pathological} + F_{pathological}} \times 100 \tag{3.4}$$

$$SP\% = \frac{T_{healthy}}{T_{healthy} + F_{healthy}} \times 100 \tag{3.5}$$

$$CC\% = \frac{T_{pathological} + T_{healthy}}{N_{pathological} + N_{healthy}} \times 100 \tag{3.6}$$

where $T_{pathological}$ is the number of true classifications of pathological case into pathological class, $T_{healthy}$, is the number of true classifications of healthy case into healthy class, $F_{pathological}$, is the number of false classifications of pathological case into the healthy class, $F_{healthy}$, is the number of false calssifications of a healthy case into the pathoşogical class, $N_{pathological}$ is the number of pathological subjects and $N_{healthy}$ is the number of healthy subjects. Thus we can write as,

- *Sensitivity ($S\%$) :* number of pathological subjects classified correctly / total number of pathological subjects.
- *Specificity ($SP\%$) :* number of healthy subjects classified correctly /total number of healthy subjects.

- *Accuracy (CC%) :* number of subjects correctly classified / total number of subjects.

Performance of four classification methodologies performed using different analysis and classification approaches are displayed in Figure 3.53, Figure 3.54 and Figure 3.55 for different k values, k=1,3 and 5. In addition to that, Figure 3.56, Figure 3.57 and Figure 3.58, related to inspiration, expiration and full cycle, respectively, are depicted to compare classifiers success in term of sensitivity and specificty. Results for each k value represented by a single point, and named with k value as 1, 3 or 5. In the figures,

- **QF1** means the quantile frequency model with k-NN using Euclidian distance measure, where feature vectors consists of cycle based quantile frequencies.
- **QF2** means quantile frequency model with k-NN using Euclidian distance measure, where feature vectors consists of segment based quantile frequencies.
- **AR1** means AR parameter model with k-NN using Euclidian distance measure.
- **AR2** means AR parameter model with k-NN using Itakura distance measure.

In **QF1** classification results were obtained separately for inspiration, expiration phases and for full respiration cycle. In classification feature vector set are formed by vectors of 4 quantile frequency values, f25, f50, f75 and f90, each vector representing a channel of one subject. Thus k-NN classification used channel data to decide the class of this channel. To obtain the class, healthy or pathological, of any subject voting method is applied based on channel classification results. For example, if subject X, for inspiration, as the result of kNN classification had five channels classified as pathological and eighth channels as healthy, voting method resulted that the subject is healthy in inspiration phase. In full cycle classification, voting took place over inspiration and expiration together, thus the decision was made by voting over 24 channels, 12 belonging to inspiration, 12 to expiration.

In **QF2** classification results were obtained as in **QF1** separately for inspiration, expiration phases and for full respiration cycle. This time, feature vector set is formed by vectors of 4 quantile frequency values, f25, f50, f75 and f90, each vector representing a segment of one channel of one subject, belonging to a specific respiratory phase. Thus k-

NN classification used channel data to decide the class of each segment. In this method two voting step were applied. First voting had classified the channel by voting between the results of its 30 segments. To obtain the class, healthy or pathological, of any subject second voting method is applied based on channel classification results. In inspiration and expiration phases only segments belonging to each phase are considered. In classification based on full respiratory cycle, first voting based on segment classification results was performed over 60 segments, representing one whole respiratory cycle, inspiration and expiration, and it produced channel classification results. Second voting step was for subject classification and was done by voting over classified 12 channels.

AR1 and **AR2** were similar by means of voting methods and what feature vector represented with **QF2** method. Only the distance metric of k-NN classifiers were different, Euclid and Itakura.

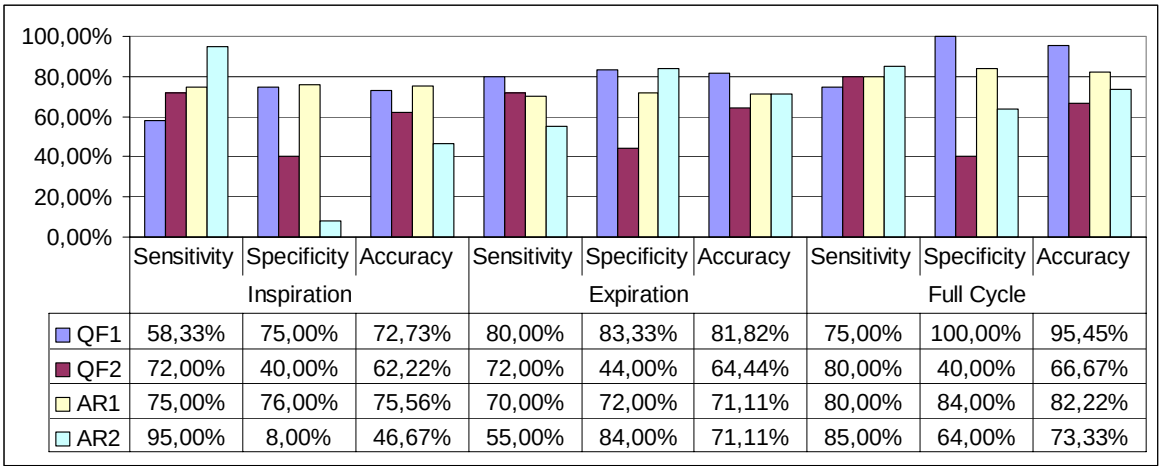

	Inspiration			Expiration			Full Cycle		
	Sensitivity	Specificity	Accuracy	Sensitivity	Specificity	Accuracy	Sensitivity	Specificity	Accuracy
QF1	58,33%	75,00%	72,73%	80,00%	83,33%	81,82%	75,00%	100,00%	95,45%
QF2	72,00%	40,00%	62,22%	72,00%	44,00%	64,44%	80,00%	40,00%	66,67%
AR1	75,00%	76,00%	75,56%	70,00%	72,00%	71,11%	80,00%	84,00%	82,22%
AR2	95,00%	8,00%	46,67%	55,00%	84,00%	71,11%	85,00%	64,00%	73,33%

Figure 3.53. Performance of classifiers for k=1

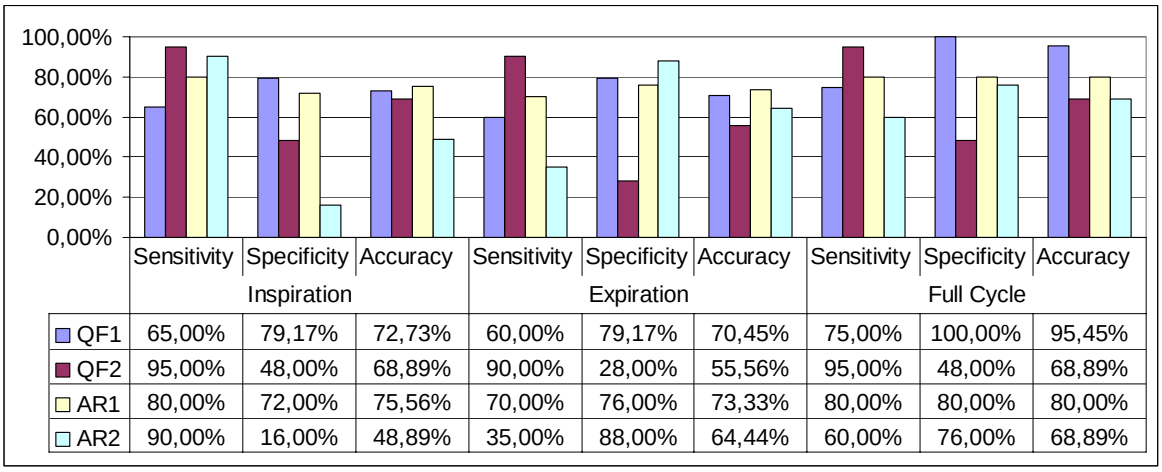

	Inspiration			Expiration			Full Cycle		
	Sensitivity	Specificity	Accuracy	Sensitivity	Specificity	Accuracy	Sensitivity	Specificity	Accuracy
QF1	65,00%	79,17%	72,73%	60,00%	79,17%	70,45%	75,00%	100,00%	95,45%
QF2	95,00%	48,00%	68,89%	90,00%	28,00%	55,56%	95,00%	48,00%	68,89%
AR1	80,00%	72,00%	75,56%	70,00%	76,00%	73,33%	80,00%	80,00%	80,00%
AR2	90,00%	16,00%	48,89%	35,00%	88,00%	64,44%	60,00%	76,00%	68,89%

Figure 3.54. Performance of classifiers for k=3

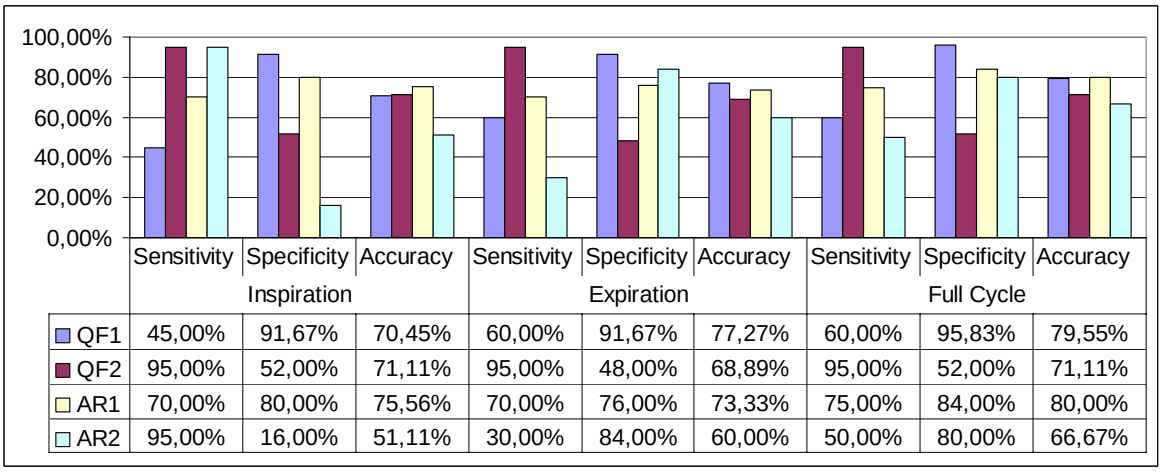

	Inspiration			Expiration			Full Cycle		
	Sensitivity	Specificity	Accuracy	Sensitivity	Specificity	Accuracy	Sensitivity	Specificity	Accuracy
QF1	45,00%	91,67%	70,45%	60,00%	91,67%	77,27%	60,00%	95,83%	79,55%
QF2	95,00%	52,00%	71,11%	95,00%	48,00%	68,89%	95,00%	52,00%	71,11%
AR1	70,00%	80,00%	75,56%	70,00%	76,00%	73,33%	75,00%	84,00%	80,00%
AR2	95,00%	16,00%	51,11%	30,00%	84,00%	60,00%	50,00%	80,00%	66,67%

Figure 3.55. Performance of classifiers for k=5

The performance of the classifier with different feature spaces is summarized. Findings can be sited as follows,

- For k=1 maximum accuracy of 81.56% of correct classification is achieved using cycle based quantile frequency parameters (QF1) in expiration whereas this figure falls to 72.73% for inspiration.
- For k=3 and k=5 maximum accuracy of approximately 75.53% of correct classification is achieved using AR parameters by Euclidian distance (AR1) in inspiration whereas this figure falls to 73.33% for expiration.

- In quantile frequency feature space (QF2), sensitivity and accuracy figures are better for inspiration whereas for AR2 vector space, sensitivity figures are better than specificity in both phases, but accuracy is lower than in QF2. For k=1 AR2 produce best results for accuracy.
- For each feature space when channels voting for subject classification performed by taking inspiration and expiration together, results for full cycle classification were obtained. For any value of k, accuracy achieved was not lower than 68.67%.
- AR2 performed better for k=1.
- In Figure 3.56 to Figure 3.58, more the point related with classifier sensitivity and specificity is near to vertical axis and farther from the horizontal axis, classifier is accepted to be better. Thus AR1 can be accepted to be the best classifier.

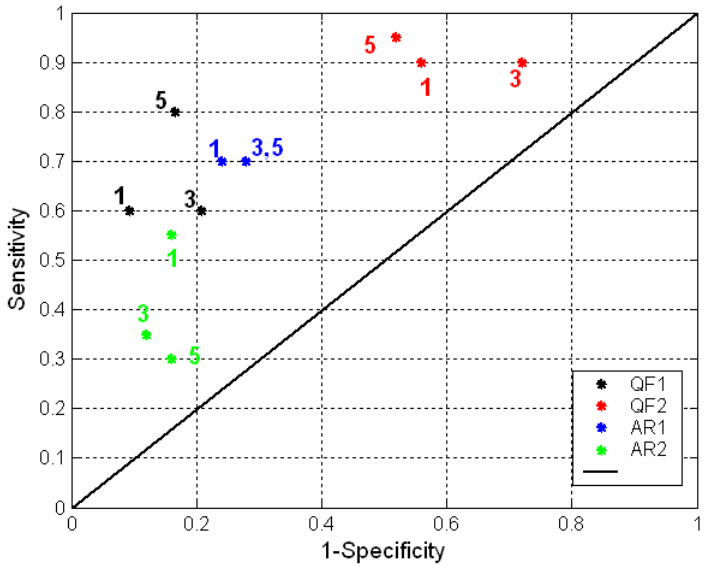

Figure 3.56. Performance of classifiers for inspiration

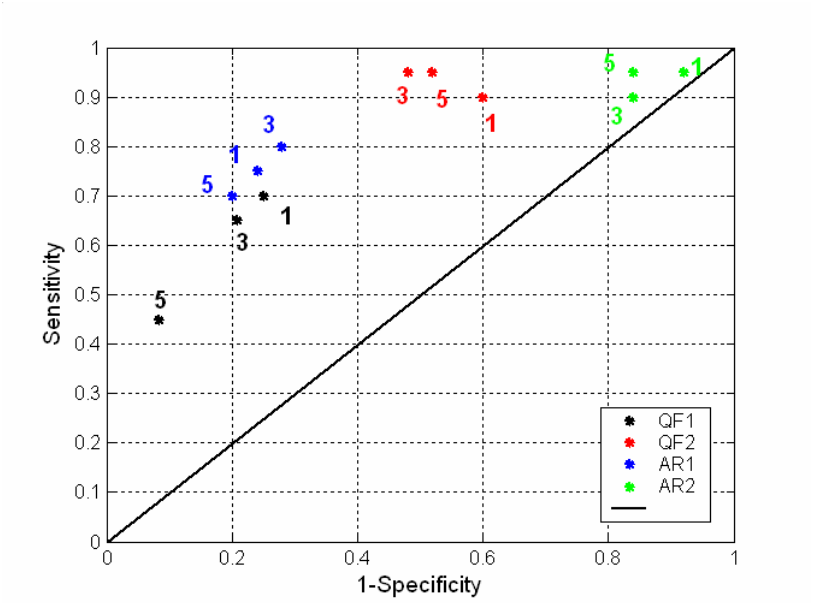

Figure 3.57. Performance of classifiers for expiration

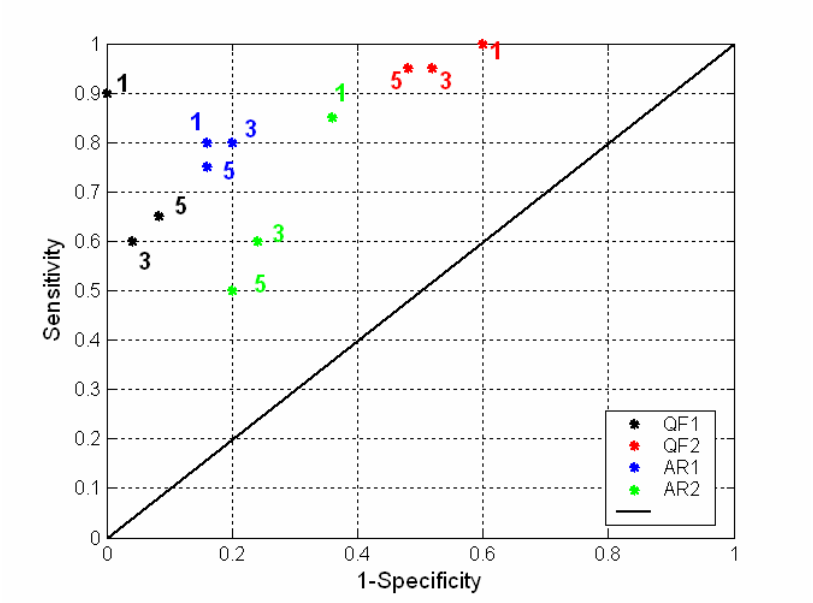

Figure 3.58. Performance of classifiers for full cycle

4. CONCLUSIONS

There is a great amount of information in lung sounds that are not evaluated or assessed by physicians. Computerized analysis can be used as an aid in the diagnosis. Moreover lung sounds provide regional information, which can be accessed more easily through a multi-channel acquisition system. This parallel lung sound recording approach also decreases the time for auscultation of 12 different locations, making it a more efficient tool.

In this study, a multi-channel k-NN classification method using two different modeling approaches, AR and power spectral analysis, were compared in the classification of respiratory sounds as healthy and pathological. The sound signal was analyzed in two phases as inspiration and expiration separately due to the nonstationarity of the signal, and classification was performed separately for each phase.

All four approaches were assessed by means of success in classifying healthy and pathological subjects. Comparison of same classifier for different k values as well as comparison of classifiers for the same k values were obtained. In all methods 12 channels were accepted to be equally weighted. In a further study, attaching different weights to different channels is expected to improve classification performance.

Further more, reference libraries corresponding to subphases, e.g., early, mid, late inspiration / expiration may be used in classification. Pathological sound signals may be further classified into specific diseases.

APPENDIX A: PATIENT PROFILE

Table A.1. Patient profile (F: female; M: male; Obs.: obstructive; Res.: restrictive)

Patient No.	Patient Name (Sex)	Age (year)	Disease Type	Clinical Diagnosis
1	Emine Kaya (F)	65	Obs.	Asthma
2	Mehmet Emin Akınay (M)	54	Obs.	Coah
3	Ali Özen (M)	66	Obs.	Coah
4	Hasref Sayir (M)	69	Obs.	Bronchiectasis
5	Mehmet Sülün (M)	45	Obs.	Coah
6	Arslan Karaca (M)	63	Obs.	Coah
7	Seyfettin Adıgüzel (M)	57	Obs.	Coah
8	Salih Gerem (M)	56	Obs.	Coah
9	Şerif Yenal (M)	37	Res.	Interstitial Lung Disease
10	Hayrettin Kaya (M)	73	Obs.	Coah
11	Esma Turan (F)	45	Obs.	Asthma+Bronchiectasis
12	Esma Gürek (F)	62	Res.	Pneumonia
13	Hulusi Ramazan (M)	67	Obs.	Coah
14	Mahmut Ayma (M)	70	Res.	Pneumonia
15	Sebahattin Kurtuldu	52	Res.	Pneumonia
16	Zülfiye Yaramaz (F)	71	Obs.	Bronchiectasis
17	Hasan Gürgan (M)	74	Res.	Interstitial Lung Disease
18	Eraydın Akkaya (M)	70	Res.	Epidermoid Lung CA
19	Giyasettin Kılıç	64	Obs.	Coah
20	Sait Avşar	50	Res.	Pneumonia

REFERENCES

1. Gavriely, N., *Breath Sounds Methodology*, Boca Radon, FL, CRC Press, 1995.

2. Pasterkamp, H., S. S. Kraman and G. R. Wodicka, "Respiratory Sounds, Advanced Beyond Stethoscope", *Am J Respir Crit Care Med*, Vol. 125, pp. 974-987, 1997.

3. Vannuccini, L., J. E. Earis, P. Helistö, B. M. G. Cheetham, M. Rossi, A. R. A. Sovijärvi and J. Vanderschoot, "Capturing and Preprocessing of Respiratory Sounds", *European Respiratory Review,* Vol. 10, No. 77, pp. 616–620, 2000.

4. Cheetham, B. M. G., G. Charbonneau, A. Giordano, P. Helisto, J. Vanderschoot, "Digitization of Data for Respiratory Sound Recordings", *European Respiratory Review,* Vol. 10, No. 77, pp. 621–624, 2000.

5. Chowdurry, S. K. and A. K. Mjumder, "Digital Spectrum of Respiratory Sounds", *IEEE Transactions on Biomedical Engineering*, BME-28, pp. 784-788, 1981.

6. Cohen, A. and D. Landsberg, "Analysis and Automatic Classification of Breath Sounds", *IEEE Transactions on Biomedical Engineering*, BME-31, pp. 585-590, 1984.

7. Iyer, V. K., A. Ramamorthy, and Y. Ploysongsang, "Autoregressive Modeling of Lung Sounds: Characterization of Source and Transmission", *IEEE Transactions on Biomedical Engineering*, Vol. 36, pp. 1133-1137, 1989.

8. Engin, T., *Solunum Seslerinin Analizi ve Sınıflandırılması*, M.S. Thesis, İstanbul Technical University, 1991.

9. Sovijärvi, A. R. A., J. Vandershoot and J. E. Earis, "Standardization of Computerized Respiratory Sound Analysis", *European Respiratory Review*, Vol.10, No. 77, pp. 585, 2000.

10. Sovijärvi, A. R. A., L. P. Malmberg, G. Charbonneau, J. Vanderschoot, F. Dalmasso, C. Sacco, M. Rossi and J. E. Earis, "Characteristics of Breath Sounds and Adventitious Respiratory Sounds", *European Respiratory Review*, Vol. 10, pp. 591–596, 2000.

11. Sovijärvi, A. R. A., F. Dalmasso, J. Vandershoot, L. P. Malmberg, G. Righini and S. A. T. Stoneman, "Definition of Terms for Respiratory Sounds", *European Respiratory Review*, Vol. 10, No. 77, pp. 597-610, 2000.

12. Earis, J. E. and B. M. G. Cheetman, "Current Method Used for Computerized Respiratory Sound Analysis", *European Respiratory Review*, Vol. 10, No. 77, pp. 641-646, 2000.

13. Sen, I. and Y. P. Kahya, "A Multi-Channel Device for Respiratory Sound Data Acquisition and Transient Detection", *Proceedings of the 2005 IEEE, Engineering in Medicine and Biology 27th Annual Conference*, Shangai, China, September 1-4, 2005.

14. Vanderschoot, J. and H. J. W. Schreur, "Flow and Volume Related AR-Modeling of Lung Sounds", *IEEE Transactions on Biomedical Engineering*, Vol. 13, pp. 385-386, 1991.

15. Guler, E. C., Observation, *Parametric Modelling and Classification of Respiratory Sounds*, M.S. Thesis, Boğaziçi University, 1992.

16. Cohen, A., *Biomedical Signal Processing*, Florida, USA, CRC Press, 1986.

17. Marple, S. L., *Digital Spectral Analysis*, Orincon Corp., San Diego, California, Prentice Hall, 1987.

18. Duda, R. O. and P. E. Hart, *Pattern Classification and Scene Analysis,* Wiley-interscience, 1973.

19. Alsmadi, S., *A DSP based instrument for real-time classification of pulmonary sounds*, M.S. Thesis, Boğaziçi University, 2003.

20. Sankur, B., Y. P. Kahya, E. C. Guler and T. Engin, "Comparison of AR-Based Algorithms for Respiratory Sounds Classifications," *Comput. Biol. Med*., Vol. 24, pp. 67-76, 1994.

21. Sen, I., *A Multi-channel Device for Respiratory Sound Data Acquisition and Transient Detection*, M.S. Thesis, Boğaziçi University, 2002.

22. Charbonneau, G., E. Ademovic, B. M. G. Cheetman, L. P. Malmberg, J. Vandershhot and A. R. A. Sovijärvi, "Basic Techniques for Respiratory Sound Analysis", *European Respiratory Review*, Vol.10, No. 77, pp. 626-635, 2000.